Frontiers of Information Technology & Electronic Engineering
www.jzus.zju.edu.cn; engineering.cae.cn; www.springerlink.com
ISSN 2095-9184 (print); ISSN 2095-9230 (online)
E-mail: jzus@zju.edu.cn

Optimal two-impulse space interception with multiple constraints*

Li XIE‡[1], Yi-qun ZHANG[2], Jun-yan XU[2]

[1]*State Key Laboratory of Alternate Electrical Power System with Renewable Energy Sources, School of Control and Computer Engineering, North China Electric Power University, Beijing 102206, China*

[2]*Beijing Institute of Electronic Systems Engineering, Beijing 100854, China*

E-mail: lixie@ncepu.edu.cn; yiqunzhang@hotmail.com; junyan_Xu@sina.cn

Received Dec. 5, 2018; Revision accepted Aug. 12, 2019; Crosschecked Mar. 6, 2020

Abstract: We consider optimal two-impulse space interception problems with multiple constraints. The multiple constraints are imposed on the terminal position of a space interceptor, impulse and impact instants, and the component-wise magnitudes of velocity impulses. These optimization problems are formulated as multi-point boundary value problems and solved by the calculus of variations. Slackness variable methods are used to convert all inequality constraints into equality constraints so that the Lagrange multiplier method can be used. A new dynamic slackness variable method is presented. As a result, an indirect optimization method is developed. Subsequently, our method is used to solve the two-impulse space interception problems of free-flight ballistic missiles. A number of conclusions for local optimal solutions have been drawn based on highly accurate numerical solutions. Specifically, by numerical examples, we show that when time and velocity impulse constraints are imposed, optimal two-impulse solutions may occur; if two-impulse instants are free, then a two-impulse space interception problem with velocity impulse constraints may degenerate to a one-impulse case.

Key words: Space interception problems; Variational method; Multiple constraints; Two-velocity impulses; Multi-point boundary value problems; Local optimal solutions; Dynamic slackness variable method
https://doi.org/10.1631/FITEE.1800763 **CLC number:** O232

1 Introduction

It is well known that from the first-order necessary optimality condition, the calculus of variations (i.e., variational methods) can be used to transform an optimization problem into a two-point or multi-point boundary value problem. Bryson (1980) told such a story about how the calculus of variations was involved in the aerospace field through the maximum range problem of a Hughes air-to-air missile in 1952. Using variational methods to solve aerospace problems can be traced back to the rocket age (Bryson, 1996). For example, in 1927, Hamel formulated the well-known Goddard problem, i.e., optimizing the altitude of a rocket given the amount of propellant, as a variational problem. Tsien and Evans (1951) reconsidered Hamel's variational problem and gave an important analytical solution and numerical data for two kinds of aerodynamic drags. A number of illustrated examples for the application of variational methods to aerospace problems have been provided in optimal control text books, e.g., Lawden (1964), Bryson and Ho (1975), Subchan and Żbikowski (2009), Ben-Asher (2010), and Longuski et al. (2014). In this study, using the calculus of variations, we solve space interception problems with multiple constraints.

‡ Corresponding author

* Project supported by the National Natural Science Foundation of China (No. 61374084)

ORCID: Li XIE, https://orcid.org/0000-0002-5214-9769

The interception problem of spacecraft is a typical aerospace problem, specifically a space maneuvering problem, in which an interceptor engaging a target in the exoatmosphere should be maneuvered to approach the target such that at impact time, their position vectors are equal. A spacecraft is normally propelled by continuous thrusts to realize a space maneuver. To simplify analysis, a continuous thrust may be approximated by an impulsive thrust when the duration of the thrust is far less than the intervals between thrusts or the coasting time of a spacecraft. It is also supposed that at a time instant when an impulsive thrust is applied, the position of a spacecraft is fixed, and its velocity changes by a jump; see, for example, Luo et al. (2007), Prussing (2010), and Curtis (2014). In this sense, we talk about a velocity impulse instead of an impulsive thrust. Using velocity impulses to approximate continuous thrusts and then obtain an optimal solution is the first step in solving a practical interception problem.

In 1925, Hohmann conceived the idea of velocity impulse and first presented the well-known two-impulse optimal orbit transfer between two circular coplanar space orbits, which is now called the Hohmann transfer. During the 1960s, the subject of impulsive trajectories including interception, transfer, and rendezvous, received much attention (Robinson, 1967; Gobetz and Doll, 1969). Using variational methods, Lawden (1964) investigated the optimal control problem of spacecraft in an inverse square law field. The primer vector theory was then specifically developed for impulsive trajectories, and a set of necessary conditions for local optimal solutions was presented; see also Jezewski (1975) and Prussing (2010). The primer vector theory was extended to incorporate final time constraints and path constraints for optimal impulsive orbital interception problems by Vinh et al. (1990) and Taur et al. (1995), respectively. It was also applied to multiple impulse orbit rendezvous; see, for example, Prussing and Chiu (1986), Colasurdo and Pastrone (1994), and Sandrik (2006). For a linear system, Prussing (1995) showed the sufficiency of these necessary conditions for an optimal trajectory. Luo et al. (2010) provided an interactive optimization approach for optimal impulsive rendezvous using the primer vector theory and evolutionary algorithms.

In the Chinese literature, the issue of space interception was also addressed in the 1970s and 1980s (Han, 1977; Qin and Wang, 1977; Cheng, 1987). In particular, Qin and Wang (1977) analytically considered an optimal one-impulsive space interception problem with an initial time as its impulse instant using variation methods based on the approximated relative motion equations of spacecraft to overcome the difficulty of numerical computation.

In our scenario, an interceptor and a target as spacecraft are assumed to be in an inverse square law field without considering other factors, e.g., aerodynamic drags. The interceptor has two opportunities to adjust its trajectory using two unknown velocity impulses to hit the target and satisfy all constraints simultaneously. The initial position and velocity vectors of both interceptors and targets are given. Then during the period without velocity impulses, the interceptor moves in free flight, as the target does. In addition to the interception constraint, we introduce the following multiple constraints that the interceptor must satisfy. The first kind of constraints is the terminal position constraint of the interceptor at an unknown terminal time, the second is a set of time constraints related to an impact time and impulse instants at which velocity impulses are applied, and the third meaningful constraint is the component-wise magnitude constraint on velocity impulses. With these constraints, two-impulse space interception problems are defined. We then formulate them as minimum-fuel optimization problems with equality or inequality constraints. A dynamic slackness variable method is developed to convert the component-wise inequality constraints on the terminal position of an interceptor into equality constraints. By the calculus of variations, a set of necessary conditions for local optimal solutions is established which finally leads to multi-point boundary value problems with unknown impulse and impact instants as well as velocity impulses. As a result, we obtain an indirect optimization method for two-impulse space interception problems with multiple constraints.

When ballistic missiles pass through the atmosphere during their flight, they have the same dynamics as spacecraft. Hence, the two-impulse interception problems of free-flight ballistic missiles can be considered as a special kind of the two-impulse space interception problems proposed in this study. We then use the indirect optimization method developed to solve the two-impulse interception

problems of free-flight ballistic missiles. The corresponding boundary value problems do not have closed-form analytic solutions, so we employ the MATLAB boundary value problem solvers bvp4c and bvp5c to numerically solve them. These two solvers that can deal with multi-point boundary value problems with unknown parameters are essentially based on the difference method, collocation, and residual control (Kierzenka, 1998; Kierzenka and Shampine, 2001, 2008; Shampine et al., 2003). The impulse and impact instants, first as unknown interior or terminal time instants, are converted into unknown parameters by a time change technique. Then we obtain the multi-point boundary value problems with unknown parameters including the components of velocity impulses, which can be solved by the MATLAB solvers and are equivalent to the original multi-point boundary value problems directly derived by the calculus of variations. A number of conclusions have been established based on the high accuracy of numerical solutions. For example, when time and velocity impulse constraints are imposed, optimal two-impulse solutions may occur.

Compared to direct optimization methods, variational methods as indirect methods provide highly accurate solutions (Ben-Asher, 2010), although extra initial conditions from costates are needed. This was also verified by numerical examples in Xie et al. (2018), where for the Hohmann transfer, the numerical solutions provided by the calculus of variations and MATLAB solvers were almost equal to analytical solutions (the global optimality of the Hohmann transfer also follows from a direct comparison of two feasible solutions instead of two strict local minima in Xie et al. (2018)). Hence, the calculus of variations is particularly suitable for investigating the properties of numerical solutions. It is possible that the interception problems could be formulated as static constrained optimization problems, because the trajectory of a spacecraft in free flight is a conic section. However, taking advantages of the calculus of variations and MATLAB solvers, we formulate them as dynamic constrained optimization problems. In addition, because of the dynamics of a spacecraft, we do not need to determine the shape of a conic section (circle, ellipse, parabola, or hyperbola). As usual, the calculus of variations and the MATLAB solvers provide local optimal solutions (see numerical examples in Xie et al. (2018)).

The organization of this paper is as follows. In Section 2, three two-impulse space interception problems with equality or inequality constraints are introduced. In Section 3, we consider the interception problems with equality constraints, i.e., Problems 1 and 2. A detailed derivation of necessary conditions for a special case of Problem 1 is presented in Appendix A to illustrate how the calculus of variations works, and boundary conditions (BCs) are also given. To convert inequality constraints into equality constraints, two slackness variable methods are presented in Section 4, and then the resulting boundary conditions for Problem 3 are obtained. The remaining parts are dedicated to solve the two-impulse interception problems of free-flight ballistic missiles. In Sections 5–8, using three sets of initial ballistic missile data, the solution properties of these particular two-impulse space interception problems are characterized and a number of numerical examples are used to illustrate our methods. Conclusions are drawn in Section 9. BCs, parameters, and initial values for Examples 2 and 3 are shown in Appendix B. Three sets of initial data for ballistic missiles are given in Appendix C. A time change technique is introduced in Appendix D.

Throughout the paper, we use boldface to denote vectors, and the subscripts M and T are used to denote the interceptor and target, respectively. The units of position and velocity are meters (m) and meters per second (m/s), respectively.

2 Problem statement

Consider the motion of a spacecraft in the Earth-centered inertial frame with the inverse square gravitational field. The state equation with the force of Earth's gravity is

$$\begin{cases} \dot{\boldsymbol{r}} = \boldsymbol{v}, \\ \dot{\boldsymbol{v}} = -\dfrac{\mu}{r^3}\boldsymbol{r}, \end{cases} \tag{1}$$

where $\boldsymbol{r}(t)$ is the spacecraft position vector, $\boldsymbol{v}(t)$ is its velocity vector, r is the magnitude of $\boldsymbol{r}(t)$, and μ is the gravitational constant 3.986×10^{14}. State vector $\boldsymbol{x}(t)$ consists of $\boldsymbol{r}(t)$ and $\boldsymbol{v}(t)$. Let an interceptor and a target be spacecraft with the dynamics defined by Eq. (1). We consider only the force of Earth's gravity and omit other factors in Eq. (1).

Problem 1 (Two-impulse space interception problem) Given the initial time t_0 and initial states

$\boldsymbol{x}_{\mathrm{M}}(t_0)$ and $\boldsymbol{x}_{\mathrm{T}}(t_0)$, after t_0, the motion of the target is described by Eq. (1). Consider two unknown time instants t_1 and t_2 such that $t_0 \le t_1 \le t_2$. Let t^+ signify time instants just after t and t^- signify time instants just before t. To guarantee that the interceptor meets the target at an unknown impact time $t_h \ge t_2$, we impose the following equality constraint on the position vectors of the interceptor and the target:

$$\boldsymbol{g}_h := \boldsymbol{r}_{\mathrm{M}}(t_h) - \boldsymbol{r}_{\mathrm{T}}(t_h) = \boldsymbol{0}, \tag{2}$$

which is historically called the interception condition of interception problems. Suppose that for the interceptor, there are velocity impulses $\Delta\boldsymbol{v}_i$

$$\boldsymbol{v}_{\mathrm{M}}(t_i^+) = \boldsymbol{v}_{\mathrm{M}}(t_i^-) + \Delta\boldsymbol{v}_i, \quad i = 1, 2. \tag{3}$$

Also the position vector $\boldsymbol{r}(t)$

$$\boldsymbol{r}_{\mathrm{M}}(t_i^+) = \boldsymbol{r}_{\mathrm{M}}(t_i^-), \quad i = 1, 2 \tag{4}$$

is continuous at the impulse instants. At continuous time instants, the state of the interceptor evolves over time according to Eq. (1). The two-impulse space interception problem as a minimum-fuel optimization problem is to design $\Delta\boldsymbol{v}_i$'s that minimize the cost functional

$$J = |\Delta\boldsymbol{v}_1| + |\Delta\boldsymbol{v}_2| \tag{5}$$

subject to constraints (2)–(4). There are three time instants: impulse instants t_1, t_2 and impact time t_h to be determined. When there is only one velocity impulse, it is called a one-impulse space interception problem.

In control theory, such an optimization problem is called an impulse control problem, in which there are state or control jumps (see, for example, Wang et al. (2014) and references therein). Indeed there is no traditional continuous-time control variable in Problem 1, but instead, the unknown velocity impulses can be viewed as control input parameters defined at discrete-time instants. It can also be considered as an example of switched or hybrid systems with interior point constraints (see, for example, Bryson and Ho (1975), Sigal and Ben-Asher (2014), Wang et al. (2014), and references therein). Next we consider a two-impulse space interception problem with a terminal position constraint on $\boldsymbol{r}_{\mathrm{M}}(t)$.

Problem 2 (Two-impulse space interception problem with a terminal position constraint) Consider a situation similar to Problem 1. Let an unknown terminal time $t_{\mathrm{f}} \ge t_h$. Define a terminal constraint on $\boldsymbol{r}_{\mathrm{M}}(t_{\mathrm{f}})$:

$$\boldsymbol{g}_{\mathrm{f}} := \boldsymbol{r}_{\mathrm{M}}(t_{\mathrm{f}}) - \boldsymbol{r}_{\mathrm{f}} = \boldsymbol{0}, \tag{6}$$

where t_{f} is to be determined and the reference position vector $\boldsymbol{r}_{\mathrm{f}} = \left[r_{\mathrm{f}x}, r_{\mathrm{f}y}, r_{\mathrm{f}z}\right]^{\mathrm{T}}$ is given in the exoatmosphere. The two-impulse space interception problem with a terminal position constraint is to design $\Delta\boldsymbol{v}_i$'s that minimize the cost functional (5) subject to constraints (2)–(4) and (6).

From a practical perspective, once an interceptor misses a target for unknown disturbances, the terminal position constraint guarantees that the interceptor is in the desired position at a final time. On the other hand, we will see that by numerical examples, the terminal position constraint can change the impact point of an interception task. We now propose a two-impulse space interception problem with multiple constraints in terms of inequalities.

Problem 3 (Two-impulse space interception problem with multiple constraints) Consider a situation similar to Problem 2. We have the following multiple constraints:

1. Instead of the equality constraint (6), inequality constraints on the terminal position $\boldsymbol{r}_{\mathrm{M}}(t_{\mathrm{f}})$ are imposed:

$$\begin{cases} r_{\mathrm{M}x}(t_{\mathrm{f}}) - r_{\mathrm{f}x} - r_{x\max} \le 0, \\ -\left(r_{\mathrm{M}x}(t_{\mathrm{f}}) - r_{\mathrm{f}x}\right) + r_{x\min} \le 0, \\ r_{\mathrm{M}y}(t_{\mathrm{f}}) - r_{\mathrm{f}y} - r_{y\max} \le 0, \\ -\left(r_{\mathrm{M}y}(t_{\mathrm{f}}) - r_{\mathrm{f}y}\right) + r_{y\min} \le 0, \\ r_{\mathrm{M}z}(t_{\mathrm{f}}) - r_{\mathrm{f}z} - r_{z\max} \le 0, \\ -\left(r_{\mathrm{M}z}(t_{\mathrm{f}}) - r_{\mathrm{f}z}\right) + r_{z\min} \le 0, \end{cases} \tag{7}$$

where $\boldsymbol{r}_{\mathrm{M}}(t_{\mathrm{f}}) = \left[r_{\mathrm{M}x}, r_{\mathrm{M}y}, r_{\mathrm{M}z}\right]^{\mathrm{T}}$ and constants $r_{x\min}$, $r_{x\max}$, $r_{y\min}$, $r_{y\max}$, $r_{z\min}$, and $r_{z\max}$ are given.

2. Time constraints on time instants t_1, t_2, and t_h are made:

$$\begin{cases} \alpha - t_1 \le 0, \quad t_1 - \beta \le 0, \\ \gamma - (t_2 - t_1) \le 0, \quad \eta - (t_h - t_2) \le 0, \end{cases} \tag{8}$$

where time constants α, β, γ, $\eta \ge 0$ are given.

3. There are component-wise inequality

constraints on velocity impulses:

$$\begin{cases} \boldsymbol{v}_1 = \left[v_{1x}, v_{1y}, v_{1z}\right]^{\mathrm{T}},\ \boldsymbol{v}_2 = \left[v_{2x}, v_{2y}, v_{2z}\right]^{\mathrm{T}}, \\ v_{1x} \in [p_{1\,\min}, p_{1\,\max}],\ v_{1y} \in [p_{2\,\min}, p_{2\,\max}], \\ v_{1z} \in [p_{3\,\min}, p_{3\,\max}],\ v_{2x} \in [p_{4\,\min}, p_{4\,\max}], \\ v_{2y} \in [p_{5\,\min}, p_{5\,\max}],\ v_{2z} \in [p_{6\,\min}, p_{6\,\max}], \end{cases} \tag{9}$$

where all boundary points of the intervals are known.

Then the two-impulse space interception problem with multiple constraints is to design $\Delta\boldsymbol{v}_i$'s that minimize the cost functional (5) subject to constraints (2)–(4) and (7)–(9).

Similar to the terminal position constraint (6), the multiple constraints (7)–(9) come from practical requirements.

3 Necessary conditions for equality constraints

For simplicity of presentation, we derive only the first-order necessary condition using the variational method for a particular case of Problem 1, in which the first impulse instant is fixed at the initial time, i.e., $t_1 = t_0$. Hence, the related terms in Problem 1 are indexed by $0, 1$ instead of $1, 2$.

Define the augmented cost functional:

$$\begin{aligned} \tilde{J} :=& |\Delta\boldsymbol{v}_0| + |\Delta\boldsymbol{v}_1| \\ &+ \boldsymbol{q}_{v1}^{\mathrm{T}}\left[\boldsymbol{v}_{\mathrm{M}}(t_0^+) - \boldsymbol{v}_{\mathrm{M}}(t_0) - \Delta\boldsymbol{v}_0\right] \\ &+ \boldsymbol{q}_{v2}^{\mathrm{T}}\left[\boldsymbol{v}_{\mathrm{M}}(t_1^+) - \boldsymbol{v}_{\mathrm{M}}(t_1^-) - \Delta\boldsymbol{v}_1\right] \\ &+ \boldsymbol{\gamma}_h^{\mathrm{T}}\boldsymbol{g}_h(\boldsymbol{r}_{\mathrm{M}}(t_h), \boldsymbol{r}_{\mathrm{T}}(t_h)) \\ &+ \int_{t_0^+}^{t_1^-}\left[\boldsymbol{p}_{\mathrm{M}r}^{\mathrm{T}}\left(\boldsymbol{v}_{\mathrm{M}} - \dot{\boldsymbol{r}}_{\mathrm{M}}\right) + \boldsymbol{p}_{\mathrm{M}v}^{\mathrm{T}}\left(-\frac{\mu}{r_{\mathrm{M}}^3}\boldsymbol{r}_{\mathrm{M}} - \dot{\boldsymbol{v}}_{\mathrm{M}}\right)\right]\mathrm{d}t \\ &+ \int_{t_0^+}^{t_1^-}\left[\boldsymbol{p}_{\mathrm{T}r}^{\mathrm{T}}\left(\boldsymbol{v}_{\mathrm{T}} - \dot{\boldsymbol{r}}_{\mathrm{T}}\right) + \boldsymbol{p}_{\mathrm{T}v}^{\mathrm{T}}\left(-\frac{\mu}{r_{\mathrm{T}}^3}\boldsymbol{r}_{\mathrm{T}} - \dot{\boldsymbol{v}}_{\mathrm{T}}\right)\right]\mathrm{d}t \\ &+ \int_{t_1^+}^{t_h}\left[\boldsymbol{p}_{\mathrm{M}r}^{\mathrm{T}}\left(\boldsymbol{v}_{\mathrm{M}} - \dot{\boldsymbol{r}}_{\mathrm{M}}\right) + \boldsymbol{p}_{\mathrm{M}v}^{\mathrm{T}}\left(-\frac{\mu}{r_{\mathrm{M}}^3}\boldsymbol{r}_{\mathrm{M}} - \dot{\boldsymbol{v}}_{\mathrm{M}}\right)\right]\mathrm{d}t \\ &+ \int_{t_1^+}^{t_h}\left[\boldsymbol{p}_{\mathrm{T}r}^{\mathrm{T}}\left(\boldsymbol{v}_{\mathrm{T}} - \dot{\boldsymbol{r}}_{\mathrm{T}}\right) + \boldsymbol{p}_{\mathrm{T}v}^{\mathrm{T}}\left(-\frac{\mu}{r_{\mathrm{T}}^3}\boldsymbol{r}_{\mathrm{T}} - \dot{\boldsymbol{v}}_{\mathrm{T}}\right)\right]\mathrm{d}t, \end{aligned} \tag{10}$$

where vectors $\boldsymbol{q}_{v1}$, $\boldsymbol{q}_{v2}$, and $\boldsymbol{\gamma}_h$ are constant Lagrange multipliers, and Lagrange multipliers $\boldsymbol{p}_{\mathrm{M}r}$, $\boldsymbol{p}_{\mathrm{M}v}$, $\boldsymbol{p}_{\mathrm{T}r}$, and $\boldsymbol{p}_{\mathrm{T}v}$ are also called costate vectors; in particular, Lawden (1964) termed $-\boldsymbol{p}_{\mathrm{M}v}$ the primer vector. We now introduce the Hamiltonian function:

$$H_{\mathrm{M}i}(\boldsymbol{r}_{\mathrm{M}}, \boldsymbol{v}_{\mathrm{M}}, \boldsymbol{p}_{\mathrm{M}i}) := \boldsymbol{p}_{\mathrm{M}ri}^{\mathrm{T}}\boldsymbol{v}_{\mathrm{M}} - \boldsymbol{p}_{\mathrm{M}vi}^{\mathrm{T}}\frac{\mu}{r_{\mathrm{M}}^3}\boldsymbol{r}_{\mathrm{M}}, \tag{11}$$

where

$$\boldsymbol{p}_{\mathrm{M}i} = \left[\boldsymbol{p}_{\mathrm{M}ri}, \boldsymbol{p}_{\mathrm{M}vi}\right]^{\mathrm{T}}, \quad i = 1, 2.$$

Then the integrals in Eq. (10) have simplified expressions; e.g., the first integral can be rewritten as

$$\int_{t_0^+}^{t_1^-}\left(H_{\mathrm{M}1}(\boldsymbol{r}_{\mathrm{M}}, \boldsymbol{v}_{\mathrm{M}}, \boldsymbol{p}_{\mathrm{M}1}) - \boldsymbol{p}_{\mathrm{M}r1}^{\mathrm{T}}\dot{\boldsymbol{r}}_{\mathrm{M}} - \boldsymbol{p}_{\mathrm{M}v1}^{\mathrm{T}}\dot{\boldsymbol{v}}_{\mathrm{M}}\right)\mathrm{d}t.$$

Taking into account all perturbations, we can obtain the first variation of the augmented cost functional. After careful derivation, as a result of making the coefficients of the variations of all independent variables vanish, the boundary conditions related to the costates of the interceptor are derived and shown in List 1 (see Appendix A for details).

List 1: BCs related to the costates for Problem 1:

$$(1)\begin{cases} \boldsymbol{p}_{\mathrm{M}v1}(t_0^+) + \dfrac{\Delta\boldsymbol{v}_0}{|\Delta\boldsymbol{v}_0|} = \boldsymbol{0}, \\ \boldsymbol{p}_{\mathrm{M}v1}(t_1^-) + \dfrac{\Delta\boldsymbol{v}_1}{|\Delta\boldsymbol{v}_1|} = \boldsymbol{0}, \\ \boldsymbol{p}_{\mathrm{M}v1}(t_1^-) - \boldsymbol{p}_{\mathrm{M}v2}(t_1^+) = \boldsymbol{0}, \\ \boldsymbol{p}_{\mathrm{M}v2}(t_h) = \boldsymbol{0}, \\ \boldsymbol{p}_{\mathrm{M}r1}(t_1^-) - \boldsymbol{p}_{\mathrm{M}r2}(t_1^+) = \boldsymbol{0}; \end{cases}$$

$$(2)\begin{cases} -\boldsymbol{p}_{\mathrm{M}r1}^{\mathrm{T}}(t_1^-)\Delta\boldsymbol{v}(t_1) = 0, \\ \boldsymbol{p}_{\mathrm{M}r2}^{\mathrm{T}}(t_h)\left(\boldsymbol{v}_{\mathrm{M}}(t_h) - \boldsymbol{v}_{\mathrm{T}}(t_h)\right) = 0. \end{cases}$$

List 2: BCs related to the costates for Problem 2:

$$(1)\begin{cases} \boldsymbol{p}_{\mathrm{M}v1}(t_1^-) + \dfrac{\Delta\boldsymbol{v}_1}{|\Delta\boldsymbol{v}_1|} = \boldsymbol{0}, \\ \boldsymbol{p}_{\mathrm{M}v2}(t_2^-) + \dfrac{\Delta\boldsymbol{v}_2}{|\Delta\boldsymbol{v}_2|} = \boldsymbol{0}, \\ \boldsymbol{p}_{\mathrm{M}v1}(t_1^-) - \boldsymbol{p}_{\mathrm{M}v2}(t_1^+) = \boldsymbol{0}, \\ \boldsymbol{p}_{\mathrm{M}v2}(t_2^-) - \boldsymbol{p}_{\mathrm{M}v3}(t_2^+) = \boldsymbol{0}, \\ \boldsymbol{p}_{\mathrm{M}r1}(t_1^-) - \boldsymbol{p}_{\mathrm{M}r2}(t_1^+) = \boldsymbol{0}, \\ \boldsymbol{p}_{\mathrm{M}r2}^{\mathrm{T}}(t_2^-) - \boldsymbol{p}_{\mathrm{M}r3}^{\mathrm{T}}(t_2^+) = \boldsymbol{0}, \\ \boldsymbol{p}_{\mathrm{M}v3}(t_h^-) - \boldsymbol{p}_{\mathrm{M}v4}(t_h^+) = \boldsymbol{0}, \\ \boldsymbol{p}_{\mathrm{M}v4}(t_{\mathrm{f}}) = \boldsymbol{0}; \end{cases}$$

$$(2)\begin{cases} -\boldsymbol{p}_{\mathrm{M}r1}^{\mathrm{T}}(t_1^-)\Delta\boldsymbol{v}(t_1)=0, \\ -\boldsymbol{p}_{\mathrm{M}r2}^{\mathrm{T}}(t_2^-)\Delta\boldsymbol{v}(t_2)=0, \\ \left(\boldsymbol{p}_{\mathrm{M}r3}^{\mathrm{T}}(t_h^-)-\boldsymbol{p}_{\mathrm{M}r4}^{\mathrm{T}}(t_h^+)\right)\left(\boldsymbol{v}_{\mathrm{M}}(t_h)\right. \\ \quad \left.-\boldsymbol{v}_{\mathrm{T}}(t_h)\right)=0, \\ \boldsymbol{p}_{\mathrm{M}r4}^{\mathrm{T}}(t_{\mathrm{f}})\boldsymbol{v}_{\mathrm{M}}(t_{\mathrm{f}})=0. \end{cases}$$

The second group of BCs in List 1 is from the Hamiltonian conditions. Similar arguments can be applied to obtain the boundary conditions related to the costates of the interceptor for Problem 2 (List 2).

4 Necessary conditions for inequality constraints

We now give the first-order necessary condition for Problem 3 with multiple constraints in terms of inequalities. The inequality constraints should first be converted into equality constraints to use the Lagrange multiplier method. Two kinds of slackness variable methods are introduced: one is rooted in the well-known Kuhn-Tucker theorem and the other is a dynamic slackness variable method developed in this study.

4.1 Inequality constraints on time instants and velocity impulses

For inequality constraints (8) and (9), we consider only the first inequality $\alpha - t_1 \leq 0$ in the time constraint (8) for a simple presentation. Problem 1 is used to illustrate how to convert an inequality constraint into an equality constraint in light of nonlinear programming.

We now introduce the static slackness variable ϵ, which ensures that $t_1 \geq \alpha$:

$$t_1-\alpha-\epsilon^2=0 \Longrightarrow t_1-\alpha=\epsilon^2\geq 0. \tag{12}$$

For slackness variable methods, please refer to Hull (2003). Then we obtain the equality constraint (12), which can be dealt with by the Lagrange multiplier method. Define a new augmented cost functional:

$$\hat{J}=\tilde{J}+\lambda(t_1-\alpha-\epsilon^2), \tag{13}$$

where $\tilde{J}$ is the original augmented cost functional defined by Eq. (10), and λ is an unknown constant Lagrange multiplier. Then the first variation of $\hat{J}$ is calculated as

$$\delta\hat{J}=\delta\tilde{J}+\lambda\,\delta t_1-2\lambda\epsilon\,\delta\epsilon.$$

To make $\delta\epsilon$ vanish such that $\delta\hat{J}=0$, we let $\lambda\epsilon=0$ and group $\lambda\delta t_1$ into the related terms of δt_1 in $\delta\tilde{J}$, for example, in Problem 1, which yields

$$-\boldsymbol{p}_{\mathrm{M}r1}^{\mathrm{T}}(t_1^-)\Delta\boldsymbol{v}(t_1)+\lambda=0. \tag{14}$$

Eliminating the slack variable yields

$$\lambda\epsilon=0\Longrightarrow\lambda\epsilon^2=0\overset{(12)}{\Longrightarrow}\lambda(t_1-\alpha)=0. \tag{15}$$

Subsequently, the necessary conditions for the inequality constraint $\alpha - t_1 \leq 0$ are obtained in terms of the interior point boundary conditions (14) and (15), where the Lagrange multiplier λ is an unknown constant to be determined. A similar argument can be used in the case of component-wise inequality constraints on velocity impulses. Our method is actually a version of the Kuhn-Tucker theorem, where Eq. (15) is called a complementary slackness condition. However, the condition (14) is new and attributes the variational method to the two-impulse interception Problem 1.

4.2 Inequality constraints on the position vector of the interceptor

Considering the terminal position constraints (7) on $\boldsymbol{r}(t_{\mathrm{f}})$, instead of the static slackness variable method, we develop a dynamic slackness variable method. The constraint on the x-direction component $r_{\mathrm{M}x}(t_{\mathrm{f}})$ of the position vector $\boldsymbol{r}_{\mathrm{M}}(t_{\mathrm{f}})$ is used to illustrate how the dynamic slackness variable method works.

The dynamic slackness variable $\epsilon(t)$ is defined by

$$\dot{\epsilon}=\begin{cases} 0, & t\in[t_0,t_1)\cup[t_1,t_2), \\ w, & t\in[t_2,t_h)\cup[t_h,t_{\mathrm{f}}], \end{cases} \tag{16}$$

where w is an unknown variable to be optimized. Using $\epsilon(t)$, the first two inequalities in constraints (7) are converted into equality constraints as follows:

$$\begin{cases} r_{\mathrm{M}x}(t_{\mathrm{f}})-r_{\mathrm{f}x}-r_{x\max}+\epsilon^2(t_{\mathrm{f}})=0, \\ -\left(r_{\mathrm{M}x}(t_{\mathrm{f}})-r_{\mathrm{f}x}\right)+r_{x\min}+\epsilon^2(t_h^-)=0. \end{cases}$$

By adding two integrals of quadratic forms in the slackness variable ϵ and its control w and adding Lagrange multiplier terms to the original cost

functional $\tilde{J}$, the augmented cost functional $\hat{J}$ is

$$\begin{aligned}\hat{J}=\tilde{J}&+\int_{t_1^+}^{t_h^-}\left(w^2+k_3\epsilon^2\right)\mathrm{d}t+\int_{t_h^+}^{t_\mathrm{f}}\left(w^2+k_4\epsilon^2\right)\mathrm{d}t\\&+\eta_1\left(r_{\mathrm{M}x}(t_\mathrm{f})-r_{\mathrm{f}x}-r_{x\max}+\epsilon^2(t_\mathrm{f})\right)\\&+\eta_2\left(-\left(r_{\mathrm{M}x}(t_\mathrm{f})-r_{\mathrm{f}x}\right)+r_{x\min}+\epsilon^2(t_h^-)\right),\end{aligned}\tag{17}$$

where k_3, k_4 are weighting coefficients and η_1, η_2 are Lagrange multipliers. This dynamic optimization problem, in which the dynamic equation consists of Eq. (1) for the interceptor and target and combines with the slackness variable (16), can be solved by the calculus of variations. Thus, the optimal $w=-0.5p_\epsilon$ and the costate equation is given by

$$\dot{p}_\epsilon=\begin{cases}0, & t\in[t_0,t_1)\cup[t_1,t_2),\\ -2k_3\epsilon, & t\in[t_2,t_h),\\ -2k_4\epsilon, & t\in[t_h,t_\mathrm{f}].\end{cases}\tag{18}$$

In the first-order variation of $\hat{J}$, one can easily obtain the terms related to the variation of ϵ as follows:

$$\begin{cases}p_{1\epsilon}(t_0)\delta\epsilon(t_0)-p_{1\epsilon}(t_1^{-*})\delta\epsilon(t_1^{-*})+p_{2\epsilon}(t_1^{+*})\delta\epsilon(t_1^{+*}),\\ -p_{2\epsilon}(t_2^{-*})\delta\epsilon(t_2^{*-})+p_{3\epsilon}(t_2^{+*})\delta\epsilon(t_2^{+*}),\\ -p_{3\epsilon}(t_h^{-*})\delta\epsilon(t_h^{-*})+p_{4\epsilon}(t_h^{+*})\delta\epsilon(t_h^{+*})-p_{4\epsilon}(t_\mathrm{f}^{*})\delta\epsilon(t_\mathrm{f}^{*}),\end{cases}\tag{19}$$

where in the i^{th} time interval, the costate p_ϵ is denoted as $p_{i\epsilon}$ $(i=1,2,3,4)$, and symbol "$*$" indicates an optimal value.

Using equalities similar to Eq. (A2) in Appendix A, eliminating variations $\delta\epsilon$, and regrouping the terms in $\mathrm{d}\epsilon$, we have the boundary conditions for ϵ and p_ϵ:

$$\begin{cases}p_{1\epsilon}(t_0)=0, \quad p_{1\epsilon}(t_1^{-*})-p_{2\epsilon}(t_1^{+*})=0,\\ p_{2\epsilon}(t_2^{-*})-p_{3\epsilon}(t_2^{+*})=0,\\ -p_{3\epsilon}(t_h^{-*})+p_{4\epsilon}(t_h^{+*})+2\eta_2\epsilon(t_h^{-*})=0,\\ -p_{4\epsilon}(t_\mathrm{f}^{*})+2\eta_1\epsilon(t_\mathrm{f}^{*})=0,\\ \epsilon(t_1^{-*})-\epsilon(t_1^{+*})=0, \quad \epsilon(t_2^{-*})-\epsilon(t_2^{+*})=0,\\ \epsilon(t_h^{-*})-\epsilon(t_h^{+*})=0,\end{cases}$$

where the first five equalities come from making the coefficients of $\mathrm{d}\epsilon$ vanish, and the last three equalities follow from the continuity of ϵ. The relationship between the Hamiltonian function $\hat{H}$ in the new augmented system and the original H is as follows:

$$\hat{H}_i=\begin{cases}H_i, & i=1,2,\\ H_i+w^2+p_{i\epsilon}w+k_i\epsilon^2=H_i-0.25p_{i\epsilon}^2+k_i\epsilon^2, & i=3,4.\end{cases}\tag{20}$$

Applying the same arguments to the y- and z-direction components of $\boldsymbol{r}_\mathrm{M}(t_\mathrm{f})$ and considering also inequality constraints (8) and (9), we obtain complete BCs related to the costates shown in List 3, where

$$\begin{cases}\boldsymbol{p}_\epsilon=\left[p_x,p_y,p_z\right]^\mathrm{T},\\ \boldsymbol{\epsilon}=\left[\epsilon_x,\epsilon_y,\epsilon_z\right]^\mathrm{T}, \quad \boldsymbol{\epsilon}^2=\left[\epsilon_x^2,\epsilon_y^2,\epsilon_z^2\right]^\mathrm{T},\\ \boldsymbol{r}_{\min}=\left[r_{x\min},r_{y\min},r_{z\min}\right]^\mathrm{T},\\ \boldsymbol{r}_{\max}=\left[r_{x\max},r_{y\max},r_{z\max}\right]^\mathrm{T},\\ \Delta\hat{H}_1=\hat{H}_3-H_3, \quad \Delta\hat{H}_2=\hat{H}_4-H_4,\end{cases}\tag{21}$$

and η_i, λ_i, and μ_i are Lagrange multipliers for inequality constraints (7), (8), and (9), respectively. To simplify notations, symbol "$*$" denoting an optimal value has been removed in all BC lists, and the index i in $\boldsymbol{p}_\epsilon$ has been dropped.

List 3: BCs related to the costates and the inequality constraints:

(1)
$$\begin{cases}\boldsymbol{p}_{\mathrm{M}v1}(t_1^-)+\dfrac{\Delta\boldsymbol{v}_1}{|\Delta\boldsymbol{v}_1|}\\ \quad+\left[\mu_1-\mu_2,\mu_3-\mu_4,\mu_5-\mu_6\right]^\mathrm{T}=\boldsymbol{0},\\ \boldsymbol{p}_{\mathrm{M}v2}(t_2^-)+\dfrac{\Delta\boldsymbol{v}_2}{|\Delta\boldsymbol{v}_2|}\\ \quad+\left[\mu_7-\mu_8,\mu_9-\mu_{10},\mu_{11}-\mu_{12}\right]^\mathrm{T}=\boldsymbol{0},\\ \boldsymbol{p}_{\mathrm{M}v1}(t_1^-)-\boldsymbol{p}_{\mathrm{M}v2}(t_1^+)=\boldsymbol{0},\\ \boldsymbol{p}_{\mathrm{M}v2}(t_2^-)-\boldsymbol{p}_{\mathrm{M}v3}(t_2^+)=\boldsymbol{0},\\ \boldsymbol{p}_{\mathrm{M}v3}(t_h^-)-\boldsymbol{p}_{\mathrm{M}v4}(t_h^+)=\boldsymbol{0},\\ \boldsymbol{p}_{\mathrm{M}v4}(t_\mathrm{f})=\boldsymbol{0},\\ \boldsymbol{p}_{\mathrm{M}r1}(t_1^-)-\boldsymbol{p}_{\mathrm{M}r2}(t_1^+)=\boldsymbol{0},\\ \boldsymbol{p}_{\mathrm{M}r2}^\mathrm{T}(t_2^-)-\boldsymbol{p}_{\mathrm{M}r3}^\mathrm{T}(t_2^+)=\boldsymbol{0};\end{cases}$$

(2)
$$\begin{cases}-\boldsymbol{p}_{\mathrm{M}r1}^\mathrm{T}(t_1^-)\Delta\boldsymbol{v}(t_1)-\lambda_1+\lambda_2+\lambda_3=0,\\ -\boldsymbol{p}_{\mathrm{M}r2}^\mathrm{T}(t_2^-)\Delta\boldsymbol{v}(t_2)-\lambda_3+\lambda_4=0,\\ \left(\boldsymbol{p}_{\mathrm{M}r3}^\mathrm{T}(t_h^-)-\boldsymbol{p}_{\mathrm{M}r4}^\mathrm{T}(t_h^+)\right)\left(\boldsymbol{v}_\mathrm{M}(t_h)-\boldsymbol{v}_\mathrm{T}(t_h)\right)\\ \quad-\lambda_4+\Delta\hat{H}_1=0,\\ \boldsymbol{p}_{\mathrm{M}r4}^\mathrm{T}(t_\mathrm{f})\boldsymbol{v}_\mathrm{M}(t_\mathrm{f})+\Delta\hat{H}_2=0;\end{cases}$$

(3)
$$\begin{cases}\lambda_1(\alpha-t_1)=0, \quad \lambda_2(t_1-\beta)=0,\\ \lambda_3(\gamma-(t_2-t_1))=0, \quad \lambda_4(\eta-(t_h-t_2))=0;\end{cases}$$

$$(4)\begin{cases}\operatorname{diag}(\mu_1,\mu_3,\mu_5)\,(\Delta\boldsymbol{v}_1-\boldsymbol{p}_{1\max})=\boldsymbol{0},\\ \operatorname{diag}(\mu_2,\mu_4,\mu_6)\,(\boldsymbol{p}_{1\min}-\Delta\boldsymbol{v}_1)=\boldsymbol{0},\\ \operatorname{diag}(\mu_7,\mu_9,\mu_{11})\,(\Delta\boldsymbol{v}_2-\boldsymbol{p}_{2\max})=\boldsymbol{0},\\ \operatorname{diag}(\mu_8,\mu_{10},\mu_{12})\,(\boldsymbol{p}_{2\min}-\Delta\boldsymbol{v}_2)=\boldsymbol{0};\end{cases}$$

$$(5)\begin{cases}\boldsymbol{\epsilon}(t_1^+)-\boldsymbol{\epsilon}(t_1^-)=\boldsymbol{0},\quad \boldsymbol{\epsilon}(t_2^+)-\boldsymbol{\epsilon}(t_2^-)=\boldsymbol{0},\\ \boldsymbol{\epsilon}(t_h^+)-\boldsymbol{\epsilon}(t_h^-)=\boldsymbol{0},\\ \boldsymbol{p}_\epsilon(t_1^+)-\boldsymbol{p}_\epsilon(t_1^-)=\boldsymbol{0},\quad \boldsymbol{p}_\epsilon(t_2^+)-\boldsymbol{p}_\epsilon(t_2^-)=\boldsymbol{0};\end{cases}$$

$$(6)\begin{cases}-\boldsymbol{p}_\epsilon(t_h^-)+\boldsymbol{p}_\epsilon(t_h^+)\\ \quad +2\operatorname{diag}(\eta_2,\eta_4,\eta_6)\boldsymbol{\epsilon}(t_h^-)=\boldsymbol{0},\\ -\boldsymbol{p}_\epsilon(t_\mathrm{f})+2\operatorname{diag}(\eta_1,\eta_3,\eta_5)\boldsymbol{\epsilon}(t_\mathrm{f})=\boldsymbol{0},\\ \boldsymbol{p}_\epsilon(t_0)=\boldsymbol{0};\end{cases}$$

$$(7)\begin{cases}\big(\boldsymbol{r}_\mathrm{M}(t_\mathrm{f})-\boldsymbol{r}_\mathrm{f}\big)-\boldsymbol{r}_{\max}+\boldsymbol{\epsilon}^2(t_\mathrm{f})=\boldsymbol{0},\\ -\big(\boldsymbol{r}_\mathrm{M}(t_\mathrm{f})-\boldsymbol{r}_\mathrm{f}\big)+\boldsymbol{r}_{\min}+\boldsymbol{\epsilon}^2(t_h^-)=\boldsymbol{0};\end{cases}$$

$$(8)\,[\eta_1-\eta_2,\eta_3-\eta_4,\eta_5-\eta_6]^\mathrm{T}-\boldsymbol{p}_{\mathrm{M}r4}(t_\mathrm{f})=\boldsymbol{0}.$$

To obtain the BCs in List 3, for the time constraints and velocity impulse constraints, the static slackness variable method is used; for the terminal position constraints, the dynamic slackness variable method works. The first group of BCs in List 3 describes the optimal conditions of the velocity impulses with component-wise constraints and the continuous conditions of the costates. The first two boundary conditions in the second group are due to the Hamiltonian functions of Problem 1 and the time inequality constraints (8); the terms $\Delta\hat{H}_1$ and $\Delta\hat{H}_2$ defined by Eq. (21) are associated with the slackness variables at time instants t_h^- and t_f. The boundary conditions in the third and fourth groups are complementary slackness conditions dealing with the time inequality constraints (8) and component-wise magnitude constraints on velocity impulses. The remaining groups come from the component-wise constraints of the terminal position and the continuous conditions of the dynamic slackness variable and its costate. Note that the dynamic slackness variable method provides an optimal solution for the augmented cost functional $\hat{J}$.

5 One-impulse space interception problem

Beginning with this section, we use all the BCs derived in the previous sections to investigate the properties of two-impulse space interception problems of free-flight ballistic missiles.

We first consider the one-impulse space interception problem, in which there is one velocity impulse to realize an interception task. The interception problems are attacked using MATLAB boundary value problem solvers. For the initial data generated by ballistic missiles, it is found that if the first impulse instant is fixed at the initial time and the second one is free, then the optimal solution degenerates to the one-impulse case in which the optimal impulse instant is equal to the initial time in the sense of local optimality. This means that a one-impulse solution is optimal. Therefore, it is necessary to first study the one-impulse space interception problem.

Without loss of generality, we assume $t_0=0$. Fix the impulse instant t_1. Thus, we have $\delta t_1=0$ in the first variation of the cost $\tilde{J}$ (Eq. (10)). Hence, the first boundary condition in the second group of List 1 related to t_1 vanishes. Then BCs for the one-impulse space interception problem with a fixed impulse instant are obtained as follows:

$$(1)\begin{cases}\boldsymbol{p}_{\mathrm{M}v1}(t_1^-)+\dfrac{\Delta\boldsymbol{v}_1}{|\Delta\boldsymbol{v}_1|}=\boldsymbol{0},\\ \boldsymbol{p}_{\mathrm{M}v1}(t_1^-)-\boldsymbol{p}_{\mathrm{M}v2}(t_1^+)=\boldsymbol{0},\quad \boldsymbol{p}_{\mathrm{M}v2}(t_h)=\boldsymbol{0},\\ \boldsymbol{p}_{\mathrm{M}r1}(t_1^-)-\boldsymbol{p}_{\mathrm{M}r2}(t_1^+)=\boldsymbol{0};\end{cases}$$

$$(2)\;\boldsymbol{p}_{\mathrm{M}r2}^\mathrm{T}(t_h)\,\big(\boldsymbol{v}_\mathrm{M}(t_h)-\boldsymbol{v}_\mathrm{T}(t_h)\big)=0.$$

Note that the first BC in the first group of List 1 has been removed, because the one-impulse case is considered.

Three sets of initial data numerically generated by the elliptical orbits of ballistic missiles as interceptors and targets are provided in Appendix C. To use the MATLAB solvers, the impulse instant t_1 is normalized by the impact instant t_h after a time change is introduced (see Appendix D for the definition). Such a normalized non-dimensional instant is called a scaled instant. Hence, the impulse instant t_1 equals the scaled $t_1\times t_h$ seconds. Local optimal numerical solutions for each scaled $t_1=[0:0.05:0.85]$ have been obtained for initial data set I. Interception trajectories for each scaled t_1 are shown in Fig. 1, where the upward direction of trajectories is the direction of increasing time. In particular, for the fixed scaled $t_1=0.2$, the corresponding primer vector magnitude is shown in Fig. 2 (the top one). One can see that its magnitude at t_1 is equal to one and does not achieve its maximum. Hence, the necessary condition of

optimal impulsive transfers (Lawden, 1964; Prussing, 2010) is not satisfied, which implies that this impulse instant t_1 is not the optimal. The magnitude of velocity impulse and the impact instant t_h versus the scaled impulse instant t_1 are shown in Figs. 3 and 4, respectively. Obviously, with the increase of scaled t_1, the magnitude of velocity impulse strictly increases, which is consistent with our intuition.

Table 1 gives the specific data of fixed impulse instants, unknown impact instants, and amplitudes of the velocity impulse obtained by the solver bvp5c, in which we set Tolerance$= 1 \times 10^{-9}$. It is found that the larger the impulse instant t_1, the more time the computation takes. We now conclude the above numerical results with Claim 1.

Claim 1 For initial data set I, the optimal cost of the one-impulse space interception problem monotonically increases with the impulse instant t_1.

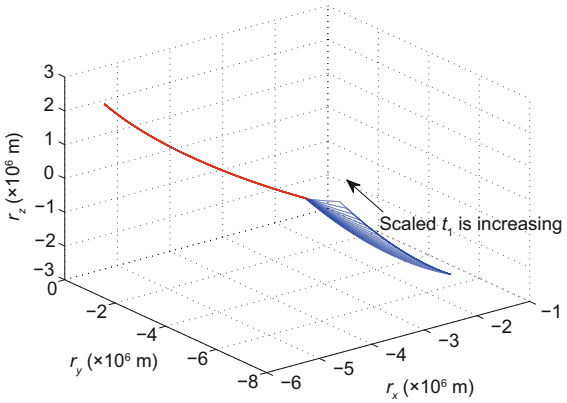

Fig. 1 Interception trajectories vs. scaled t_1

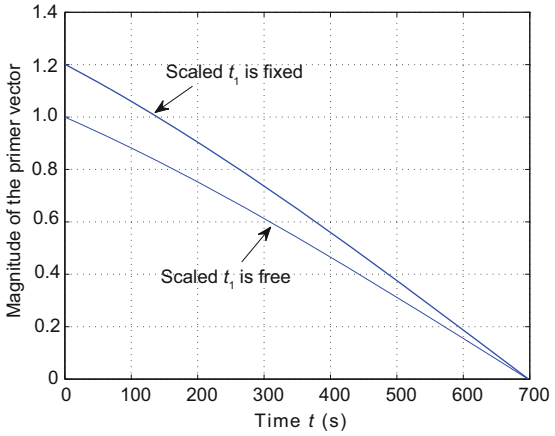

Fig. 2 Magnitude of the primer vector for scaled $t_1 = 0.2$

It follows from Table 1 and Claim 1 that the cost of the one-impulse space interception problem achieves its minimum at the initial time $t_0 = 0$. This can also be seen from solving the related boundary value problem with an unknown instant t_1 by imposing an inequality constraint $-t_1 \leq 0$ for the one-impulse case. Without this inequality constraint, the

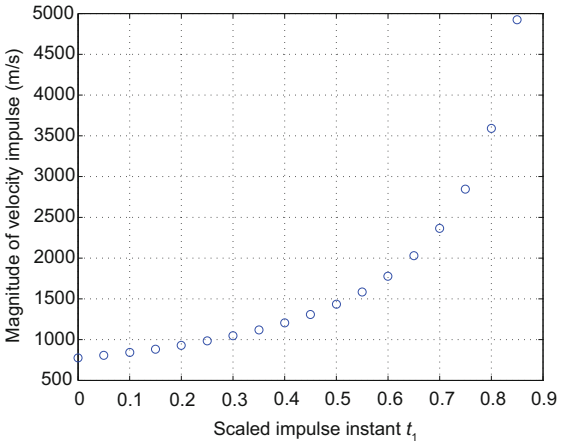

Fig. 3 Cost vs. scaled impulse instant

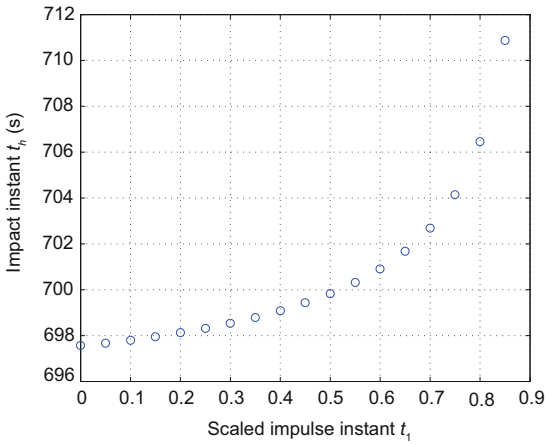

Fig. 4 Impact instant vs. scaled impulse instant

Table 1 Fixed impulse instants, impact instants, and velocity impulse magnitudes

t_1 (s)	t_h (s)	$\lvert\Delta \boldsymbol{v}_1\rvert$ (m/s)	t_1 (s)	t_h (s)	$\lvert\Delta \boldsymbol{v}_1\rvert$ (m/s)
0	697.5637	774.9142	60	697.7622	832.3724
5	697.5779	779.2491	70	697.8013	843.2137
10	697.5925	783.6609	80	697.8422	854.4603
20	697.6230	792.7212	90	697.8847	866.1314
30	697.6553	802.1083	100	697.9291	878.2470
40	697.6892	811.8358	200	698.4787	1.0295×10^3
50	697.7249	821.9186	600	710.2164	4.7368×10^3

MATLAB solver gives a negative impulse instant. This is reasonable because in the derivation of BCs by the variational method, the time constraint $t_1 \geq 0$ is not imposed. Inequality $t_1 \geq 0$ is essentially not a constraint since the time is naturally non-negative. Hence, in this sense we also say that the instant t_1 is free. List 4 shows the BCs that are obtained by the static slackness variable method (Eqs. (14) and (15)).

Claim 2 For initial data set I, the one-impulse space interception problem has a local minimum at the initial time t_0.

List 4: BCs related to the costates for free t_1:

$$(1)\begin{cases} \boldsymbol{p}_{\mathrm{M}v1}(t_1^-)+\dfrac{\Delta \boldsymbol{v}_1}{|\Delta \boldsymbol{v}_1|}=\boldsymbol{0}, \\ \boldsymbol{p}_{\mathrm{M}v1}(t_1^-)-\boldsymbol{p}_{\mathrm{M}v2}(t_1^+)=\boldsymbol{0}, \quad \boldsymbol{p}_{\mathrm{M}v2}(t_h)=\boldsymbol{0}, \\ \boldsymbol{p}_{\mathrm{M}r1}(t_1^-)-\boldsymbol{p}_{\mathrm{M}r2}(t_1^+)=\boldsymbol{0}; \end{cases}$$

$$(2)\begin{cases} -\boldsymbol{p}_{\mathrm{M}r1}^{\mathrm{T}}(t_1^-)\Delta \boldsymbol{v}(t_1)-\lambda=0, \\ \boldsymbol{p}_{\mathrm{M}r2}(t_h)\left(\boldsymbol{v}_{\mathrm{M}}(t_h)-\boldsymbol{v}_T(t_h)\right)=0; \end{cases}$$

$$(3)\ \lambda(0-t_1)=0.$$

By the BCs in List 4, the solver bvp5c with Tolerance=$2.220\,45\times10^{-14}$ gives the solution message (Table 2).

Table 2 Solution message for the one-impulse space interception problem

Item	Value
Maximum error	2.068×10^{-14}
Elapsed time (s)	132.710 440
Velocity impulse (m/s)	$[-376.7263; 338.2633; -586.6407]$
Magnitude of the velocity impulse (m/s)	774.9142
Time instant of the velocity impulse (s)	0
Impact instant (s)	697.5637
Lagrange multiplier λ	0.8594

One can see that the local optimal impulse instant exactly equals zero, which together with Claim 1 numerically verifies Claim 2. The primer vector magnitude shown in Fig. 2 (the bottom one) achieves its maximum at $t=0$, which is consistent with the necessary condition of the primer vector theory.

Remark 1 To obtain Table 1, the numerical experiments for each fixed (scaled) impulse instant t_1 are carried out under the same initial conditions including the initial state and parameter values. The first-order necessary optimal condition derived from the calculus of variations can guarantee only the local optimality of solutions. In this sense, by Claims 1 and 2, we report that the local optimal cost for the one-impulse ballistic missile interception problem has a monotonic property with respect to varying impulse instants under the same initial numerical circumstance, and hence takes a minimum at the initial instant. In the following, a local optimal solution is simply called an optimal solution. Claims 1 and 2 also hold for initial data sets II and III, which may explain why Qin and Wang (1977) directly assumed that a velocity impulse was applied at an initial time. The same conclusions are also drawn by using direct optimization methods with the help of the MATLAB software GPOPS version 5.0. Although all claims are numerically verified via three sets of initial data, our methodology can be used to investigate general situations. All numerical computations are performed on a Mac OS X system with an Intel Core i5 (2.4 GHz, 4 GB) processor. The computation time (elapsed time) is related to the initial values and the version of MATLAB. All initial values and parameters needed in the numerical examples are omitted except in some important examples.

6 Occurrence of two velocity impulses

We now examine the conditions under which two velocity impulses occur in Problem 1 for free-flight ballistic missiles. Two velocity impulses occur if impulse instants are different and neither of the two velocity impulses is equal to zero. A special case of Problem 1 where the first impulse instant is fixed at $t_0=0$ is first considered for initial data set I.

Example 1 Consider Problem 1 and initial data set I. Fix the first impulse instant t_1 at zero (i.e., $t_1=t_0=0$). Based on the BCs shown in List 1, solver bvp5c gives the solution message shown in Table 3. The maximum absolute BC error is $1.514\,481\times10^{-9}$.

Compared with the one-impulse solution in Claim 2, we can say that the local optimal two-impulse solution degenerates to the optimal one-impulse case because the order of magnitude of the scaled instant of the second impulse instant t_2 is 1×10^{-10}. Hence, one question is raised: under what conditions does a true two-impulse solution

Table 3 Solution message for the two-impulse space interception problem in Example 1

Item	Value
Maximum error	9.526×10^{-10}
Elapsed time (s)	11 689.357 989
First velocity impulse (m/s)	$[-376.7263; 338.2633; -586.6407]$
Second velocity impulse (m/s)	$1.0 \times 10^{-10} \times [-0.3026; 0.2717; -0.4713]$
Magnitude of the velocity impulse (m/s)	774.9142
Time instant of the first velocity impulse (s)	0
Scaled instant of the second velocity impulse	3.6313×10^{-10}
Impact instant (s)	697.5637

Table 4 Solution message for the two-impulse space interception problem in Example 2

Item	Value
Maximum error	2.326×10^{-14}
Elapsed time (s)	157.390 451
First velocity impulse (m/s)	$1.0 \times 10^3 \times [1.3000; -0.8802; 1.2638]$
Second velocity impulse (m/s)	$[643.4791; -334.8857; 474.7955]$
Magnitude of the velocity impulse (m/s)	2882.4177
Time instant of the first velocity impulse (s)	20
Time instant of the second velocity impulse (s)	70
Impact instant (s)	$3.982\,766 \times 10^2$

occur? We conjecture that if inequality constraints on impulse instants and the magnitudes of velocity impulses are imposed simultaneously, then two-impulse solutions may occur. This is verified in the following two examples. Here, all related inequality constraints are converted into equalities using the static slackness variable method. The corresponding BCs in this section are shown in List 5 in Appendix B.

Example 2 For initial data set III, inequality constraints are imposed component-wise on velocity impulses (9), while time constraints (8) are imposed on impulse instants:

$$\begin{cases} \alpha - t_1 \le 0, \quad t_1 - \beta \le 0, \quad \gamma - (t_2 - t_1) \le 0, \\ \alpha, \beta, \gamma \ge 0; \end{cases} \tag{22}$$

that is, $t_1 \in [\alpha, \beta], t_2 - t_1 \ge \gamma$. All parameters and initial values are shown in Table B1 (see Appendix B). Solver bvp5c gives the solution message shown in Table 4.

The interception trajectory, the velocity vector, their magnitudes, and primer vector and position costate magnitudes are shown in Figs. 5–8.

Example 3 For initial data set I, consider the same constraints as in Example 2 and set the related parameters and initial values by Table B2 in Appendix B. The solution message is shown in Table 5.

Examples 2 and 3 show that the inequality constraints component-wise on velocity impulses (9) and time constraints on impulse instants (22) may indeed result in the occurrence of a local optimal two-impulse solution.

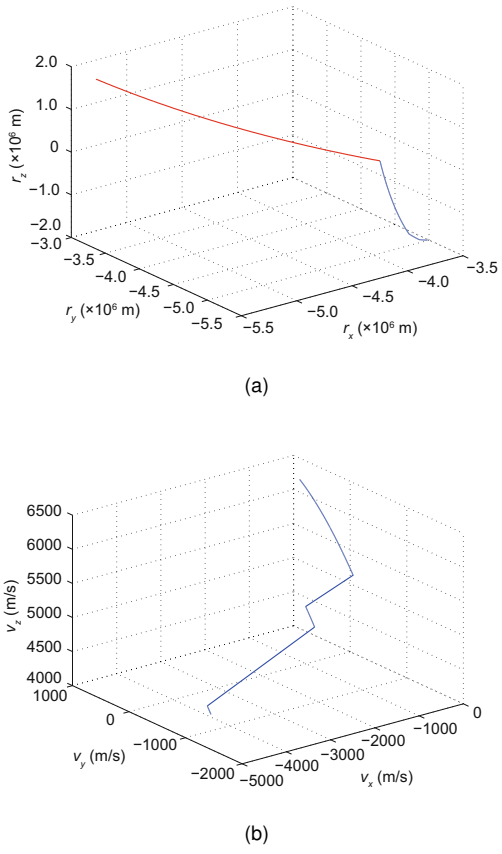

Fig. 5 Interception trajectory (a) and velocity vector of the interceptor (b) in Example 2

At the beginning of this section, it was shown that when t_1 is fixed at t_0, the two-impulse case degenerates to the one-impulse case. The next example

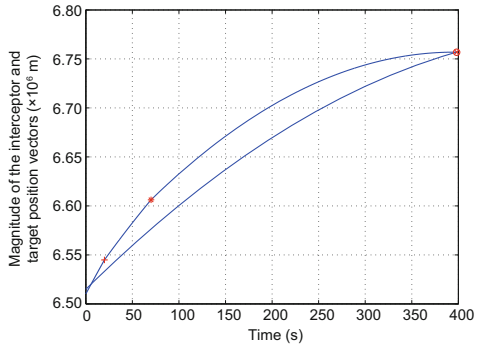

(a)

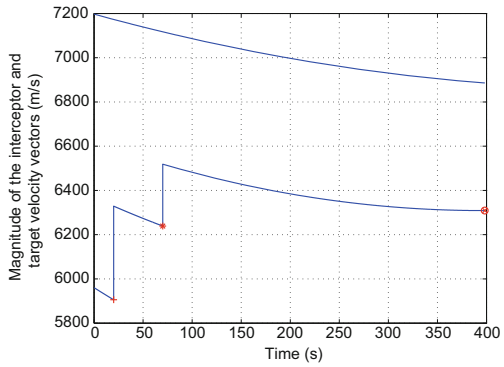

(b)

Fig. 6 Magnitude of position (a) and velocity (b) vectors in Example 2 (+ and ∗ indicate the positions of velocity impulses and ⊗ indicates the position of the impact point)

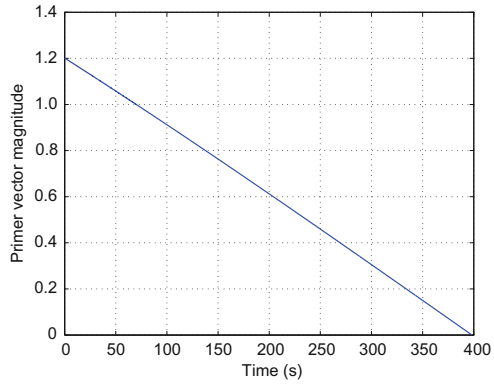

Fig. 7 Magnitude of the primer vector in Example 2

illustrates that even if there are time and velocity impulse constraints, this degeneration may still occur.

Example 4 Consider initial data set I. The component-wise magnitudes on two-velocity impulses as constraints (7) and inequality constraints on impulse instants

$$0 - t_1 \leq 0, \quad 0 - t_2 \leq 0 \tag{23}$$

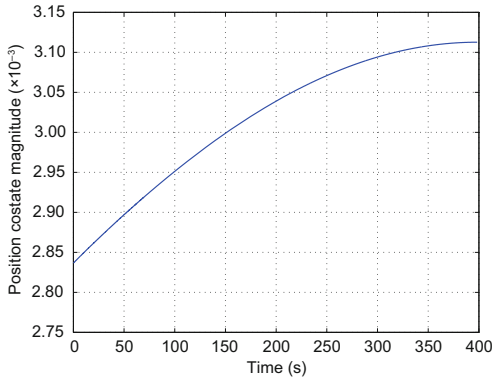

Fig. 8 Position costate magnitude of the interceptor in Example 2

Table 5 Solution message for the two-impulse space interception problem in Example 3

Item	Value
Maximum error	1.612×10^{-14}
Elapsed time (s)	98.575 404
First velocity impulse (m/s)	[−358.9788; 319.8635; −500.0000]
Second velocity impulse (m/s)	[−51.8201; 46.1877; −80.8052]
Magnitude of the velocity impulse (m/s)	800.1978
Time instant of the first velocity impulse (s)	20
Time instant of the second velocity impulse (s)	70
Impact instant (s)	$6.957\,846 \times 10^2$

are imposed, and the solution message is shown in Table 6. The local optimal impulse instants can be considered as zero because the order of magnitudes is 1×10^{-22}. Hence, the local optimal two-impulse solution is actually the solution of the one-impulse case.

Examples 2–4 reveal the following results:

1. The two impulses may occur under time and velocity impulse magnitude constraints (see Examples 2 and 3).

2. If the two impulses occur at instants t_1 and t_2, then the magnitude of the two velocity impulses is larger than that of the one-impulse case in which the velocity impulse is applied at the t_1 instant and less than that of the one-impulse case in which the velocity impulse is applied at the t_2 instant (see Example 3 and Table 1).

3. The upper and lower bounds on velocity

impulse magnitudes have effects on the optimal two-impulse solutions.

4. With time and velocity impulse magnitude constraints, if the lower bound of two-impulse instants equals zero, then the two-impulse case degenerates to the one-impulse case with the constraint $t_1 \geq 0$, and the impulse instant of both cases is equal to 0 (see Example 4).

The above conclusions are drawn from only a few numerical examples, and no theoretical proof is available. Although they seem to be consistent with physical intuitions, they still need to be verified by more numerical examples. To end this section, a conjecture for Problem 1 is presented:

Conjecture 1 For all numerical examples under consideration, the two-impulse space interception (Problem 1) is equivalent to the one-impulse case in the sense of having identical locally optimal solutions.

Unfortunately, a numerical solution cannot be found to confirm this conjecture within a valid period of time using the MATLAB solver. However, it is correct if the constraints of velocity impulses are imposed (see Example 4).

7 A terminal position constraint

We now consider two-impulse space interception problems with a terminal point constraint—Problem 2—for free-flight ballistic missiles. It is found that the two-impulse case with free impulse instants is equivalent to the one-impulse case for our examples. Hence, the one-impulse case is addressed first.

Example 5 Consider the one-impulse space interception problem with the terminal position constraint for initial data set II. The BCs can be obtained by removing the BCs related to t_2 in List 2. The solution message is given by Table 7.

For Problem 1 with initial data set II, the message of the optimal one-impulse solution is shown in Table 8.

It is obvious that in this example, the cost of Problem 1 is less than the cost of Problem 2, and the terminal position constraint indeed changes the impulse and impact instants, the cost, and the corresponding position and velocity vectors. Figs. 9–12 show the trajectories and velocity vectors of the interceptor and target. The primer vector and position costate magnitudes are given in Figs. 13 and 14, from which one can see that there is a jump at the impact instant for the position costate, and the primer vector achieves its maximal magnitude at the impulse instant t_1.

The next example shows that the two-impulse

Table 6 Solution message for the two-impulse space interception problem in Example 4

Item	Value
Maximum error	1.329×10^{-13}
Elapsed time (s)	107.589 378
First velocity impulse (m/s)	$[-222.9102; 200.1515; -347.1171]$
Second velocity impulse (m/s)	$[-153.8162; 138.1118; -239.5235]$
Magnitude of the velocity impulse (m/s)	774.9142
Time instant of the first velocity impulse (s)	$2.411\,938 \times 10^{-24}$
Time instant of the second velocity impulse (s)	$1.030\,637 \times 10^{-22}$
Impact instant (s)	$6.975\,637 \times 10^{2}$

Table 7 Solution message for the one-impulse space interception problem for Problem 2 in Example 5

Item	Value
Maximum error	1.681×10^{-14}
Elapsed time (s)	68.651 997
Velocity impulse (m/s)	$[-398.4799; 367.8786; -588.7740]$
Magnitude of the velocity impulse (m/s)	800.4847
Time instant of the velocity impulse (s)	$5.350\,987 \times 10$
Impact instant (s)	$6.824\,639 \times 10^{2}$
Terminal time (s)	$9.489\,139 \times 10^{2}$

Table 8 Solution message for Problem 1 in Example 5

Item	Value
Maximum error	2.103×10^{-14}
Elapsed time (s)	126.472 090
Velocity impulse (m/s)	$[-360.3182; 333.9543; -565.8637]$
Magnitude of the velocity impulse (m/s)	749.3707
Time instant of the velocity impulse (s)	4.1561×10^{-27}
Impact instant (s)	$6.835\,178 \times 10^{2}$

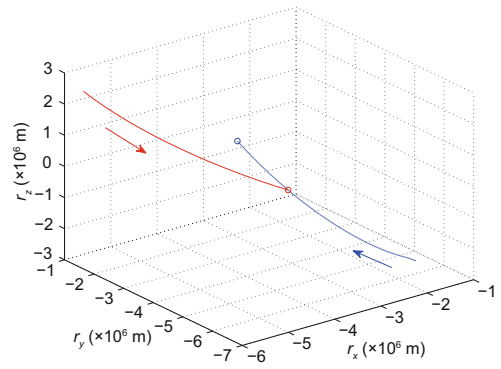

Fig. 9 Interception trajectory in Example 5 (symbol ○ corresponds to the terminal point of the interceptor)

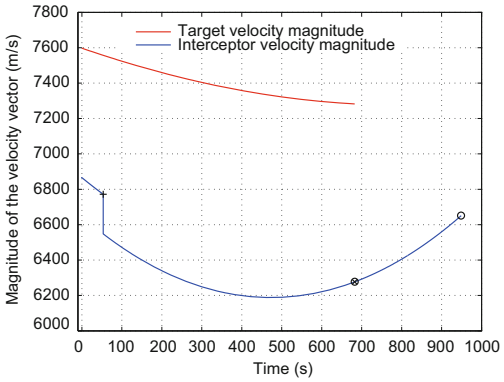

Fig. 12 Velocity vector magnitudes in Example 5 (symbol ○ corresponds to the terminal velocity vector)

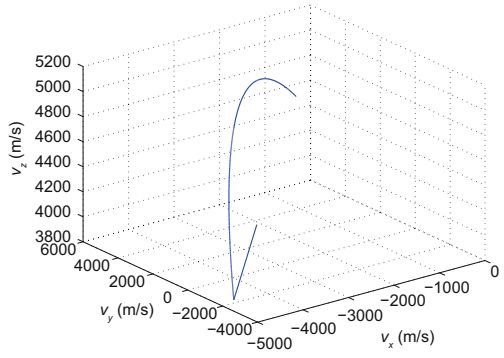

Fig. 10 Interceptor velocity vector in Example 5

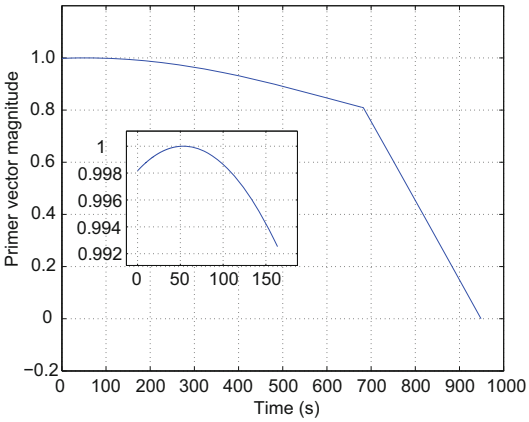

Fig. 13 Primer vector magnitude in Example 5

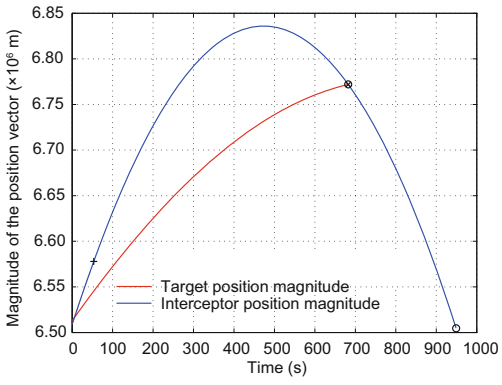

Fig. 11 Position vector magnitudes in Example 5 (symbol ○ corresponds to the terminal position vector, i.e., the reference position vector)

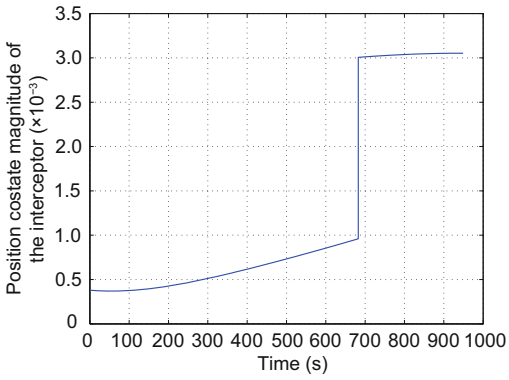

Fig. 14 Position costate magnitude of the interceptor in Example 5

space interception problem with a terminal position constraint is equivalent to the one-impulse case considered in Example 5.

Example 6 Consider initial data set II for Problem 2 of ballistic missiles. The BCs are given by List 2. The solution message is shown in Table 9.

Note that $t_2 - t_1 = 7.034\,373 \times 10^{-13}$ s, which implies that the two-impulse case degenerates to the one-impulse case.

For Problem 2, it is possible that if t_1 is fixed at

t_0, then an optimal two-impulse solution occurs.

Example 7 Consider initial data set I. The first impulse instant is fixed at zero. The two-impulse solution is given by Table 10.

The cost is slightly greater than that of the impulse instant free case, which equals 774.950 428 m/s ($t_1 = t_2 = 4.3921 \times 10^{-5}$ s, Tolerance$= 1 \times 10^{-6}$).

8 Numerical verification for multiple constraints

We know that if time and velocity impulse inequality constraints are imposed, then a local optimal two-impulse solution to Problem 1 of free-flight ballistic missiles may occur. In this section, Problem 3, where there are multiple constraints in terms of inequalities, is considered. The multiple constraints include an additional inequality constraint on the terminal position vector of the interceptor as well as time and velocity impulse inequality constraints. The static slackness variable method is used to convert the time inequality constraints and component-wise constraints on velocity impulses into equalities, and the dynamic slackness variable method is used for the terminal constraints of the interceptor's final position vector.

Table 9 Solution message for the two-impulse space interception problem in Example 6

Item	Value
Maximum error	6.284×10^{-15}
Elapsed time (s)	172.984 882
First velocity impulse (m/s)	$[-397.8985; 367.3419; -587.9150]$
Second velocity impulse (m/s)	$[-0.5813; 0.5367; -0.8589]$
Magnitude of the velocity impulse (m/s)	774.9142
Time instant of the first velocity impulse (s)	$5.350\,987 \times 10$
Time instant of the second velocity impulse (s)	$5.350\,987 \times 10$
Impact instant (s)	$6.824\,639 \times 10^2$
Terminal time (s)	$9.489\,139 \times 10^2$

Table 10 Solution message for the two-impulse space interception problem in Example 7

Item	Value
Maximum error	3.308×10^{-10}
Elapsed time (s)	837.853 649
First velocity impulse (m/s)	$[-358.2908; 321.7015; -558.0683]$
Second velocity impulse (m/s)	$[-18.3931; 16.5315; -28.6650]$
Magnitude of the velocity impulse (m/s)	774.950 445
Time instant of the first velocity impulse (s)	0
Scaled time instant of the second velocity impulse	8.9894×10^{-4}
Scaled impact instant	0.7275
Terminal time (s)	958.9110

Example 8 Consider the two-impulse ballistic missile space interception Problem 3 with initial data set II. The parameters with respect to all constraints (7)–(9) and the initial values of all unknown variables are shown in Tables 11–13. The optimal initial costate values in Problem 1 are assumed as a guess of costates as follows:

$$\mathbf{pmr0} = 1.0 \times 10^{-3}[0.2913; 0.2507; -0.0421],$$
$$\mathbf{pmv0} = [0.4861; -0.4364; 0.7571].$$

There are 116 BCs; the BCs that are related to the costates are given in List 3. Then, by trial and error, the MATLAB solver bvp5c successfully provides the solution message (shown in Table 14

Table 11 Time constraints (8) and velocity impulse constraints (9) in Example 8

Item	Value	Item	Value	Item	Value
α	20	$p_{2\,\min}$	100	$p_{5\,\min}$	100
β	30	$p_{2\,\max}$	200	$p_{5\,\max}$	500
γ	41	$p_{3\,\min}$	-100	$p_{6\,\min}$	-600
η	0	$p_{3\,\max}$	-50	$p_{6\,\max}$	-100
$p_{1\,\min}$	-200	$p_{4\,\min}$	-500		
$p_{1\,\max}$	100	$p_{4\,\max}$	-100		

Table 12 Initial ϵ, p_ϵ for Eqs. (16) and (18), constraints (7), and initial Δv in Example 8

Item	Value	Item	Value
$\epsilon_x, \epsilon_y, \epsilon_z, p_x, p_y, p_z$	1	$\mathrm{dv1}_x$	-100
$r_{x\,\min}$	-500	$\mathrm{dv2}_x$	-300
$r_{x\,\max}$	500	$\mathrm{dv1}_y$	100
$r_{y\,\min}$	-500	$\mathrm{dv2}_y$	300
$r_{y\,\max}$	500	$\mathrm{dv1}_z$	-100
$r_{z\,\min}$	-500	$\mathrm{dv2}_z$	-400
$r_{z\,\max}$	500		

Table 13 Initial scaled and final instants, weighting coefficients in Eq. (17) and Lagrange multipliers for List 3 in Example 8

Item	Value
Scaled t_1	0.02
Scaled t_2	0.04
Scaled t_h	0.14
t_f	950
$k_{3x}, k_{3y}, k_{3z}, k_{4x}, k_{4y}, k_{4z}$	1
$\lambda_1; \lambda_2, \lambda_3, \lambda_4$	1.006; 1
$\mu_1, \mu_2, \ldots, \mu_{12}$	1
$\eta_1, \eta_2, \ldots, \eta_6$	-2

Table 14 Solution message for the two-impulse space interception problem in Example 8

Item	Value
Maximum error	9.887×10^{-10}
Elapsed time (s)	3841.473 078
First velocity impulse (m/s)	$[-100; 100; -100]$
Second velocity impulse (m/s)	$[-297.2786; 265.4892; -490.6278]$
Magnitude of the velocity impulse (m/s)	805.3242
Time instant of the first velocity impulse (s)	$2.075\,471 \times 10$
Time instant of the second velocity impulse (s)	$6.175\,471 \times 10$
Impact instant (s)	$6.824\,994 \times 10^2$
Terminal time (s)	$9.491\,821 \times 10^2$
Difference between $\boldsymbol{r}_\mathrm{M}(t_\mathrm{f})$ and $\boldsymbol{r}_\mathrm{f}$ (m)	[500.000; 500.000; 500.000]

and Tolerance$= 1 \times 10^{-9}$) to Problem 3.

Figs. 15–22 show the interception trajectory, the velocity vector and their magnitudes for both the interceptor and target, the primer vector and position costate magnitudes of the interceptor, and the slackness variable and its costate in the x direction, respectively. If we use the MATLAB solver bvp4c instead, assume its tolerance to be 1×10^{-6}, set $\lambda_1 = 1.0056$, and modify the code by vectorization methods, then a solution approximately equal to the one shown in Table 14 is found, satisfying all constraints with a certain accuracy, and the computation time is about 70 s.

Note that the two-impulse space interception problem with multiple constraints cannot be solved within a valid period of time if the static slackness variable method is used for the terminal position

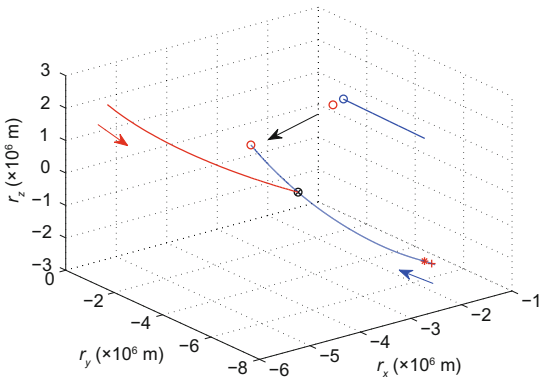

Fig. 15 Interception trajectory in Example 8 (symbols $*$ and $+$ correspond to the impulse instants, and $\circ$ and $\otimes$ correspond to the terminal instant of the interceptor and impact instant respectively)

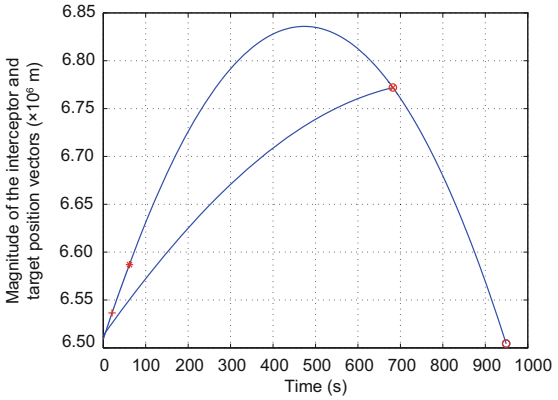

Fig. 16 Magnitude of position vectors in Example 8 (symbols $*$ and $+$ correspond to the impulse instants, and $\circ$ and $\otimes$ correspond to the terminal instant of the interceptor and impact instant respectively)

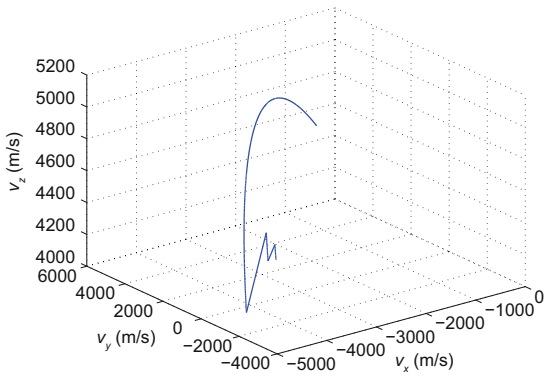

Fig. 17 Velocity vector of the interceptor in Example 8

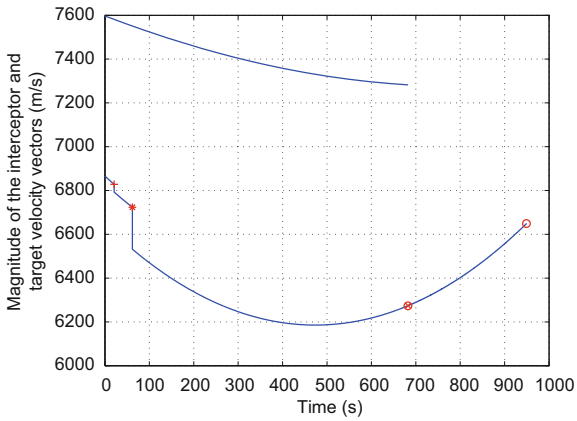

Fig. 18 Magnitude of velocity vectors in Example 8 (symbols $*$ and $+$ correspond to the impulse instants, and $\circ$ and $\otimes$ correspond to the terminal instant of the interceptor and impact instant respectively)

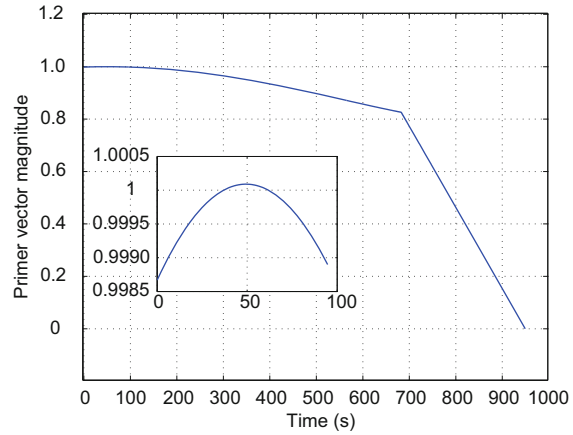

Fig. 19 Primer vector magnitude in Example 8

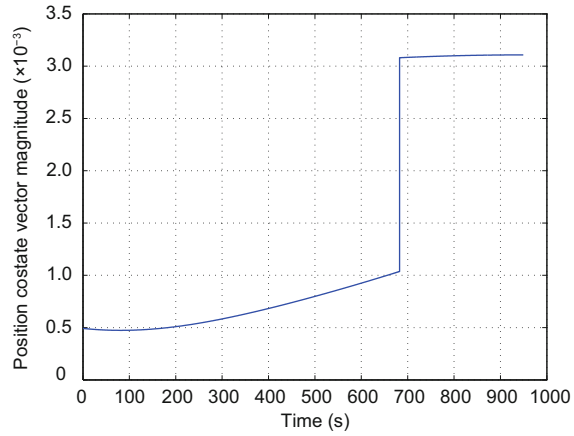

Fig. 20 Position costate magnitude of the interceptor in Example 8

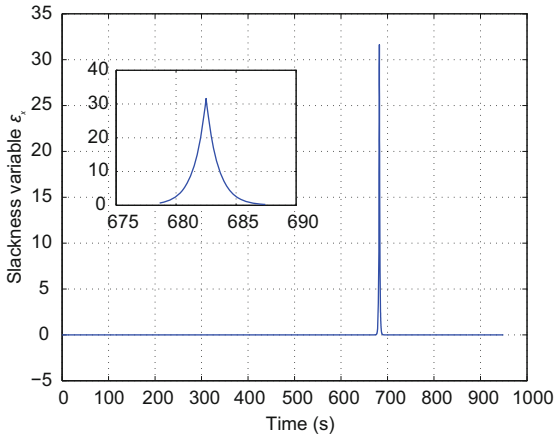

Fig. 21 Slackness variable ϵ_x in Example 8

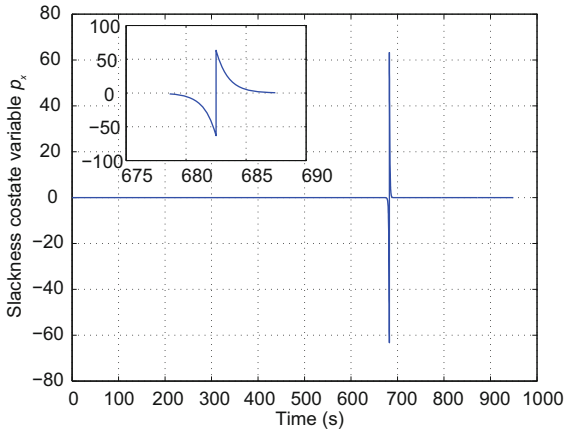

Fig. 22 Costate of the slackness variable in Example 8

inequality constraints. Instead, the dynamic slackness variable method is introduced in this study. One can see from Example 8 that the solution given by the dynamic slackness variable method satisfies all constraints. For a one-impulse space interception problem with time constraints, numerical experiments show that the magnitude of the velocity impulse obtained by the static slackness variable method can be approached from above by the one with the dynamic slackness variable method by adjusting weighting coefficients.

9 Conclusions

Using the calculus of variations, we have solved two-impulse space interception problems with multiple constraints in this paper. The multiple constraints include impulse and impact instant constraints, terminal constraints on the final position of

an interceptor, and component-wise constraints on the magnitudes of velocity impulses. A number of conclusions concerning two-impulse ballistic missile space interception problems have been established based on highly accurate numerical solutions provided by MATLAB boundary value problem solvers.

There is one question confusing us when we deal with two-impulse ballistic missile interception problems using MATLAB boundary value problem solvers; that is, under what circumstance does a true two-impulse optimal solution occur for Problem 1? By numerical examples, it is found that if the first impulse instant is fixed at the initial time and the second one is free, then its optimal solution degenerates to the one-impulse case in which the optimal impulse instant is equal to the initial time, meaning that the one-impulse solution is optimal. We then conjecture that to ensure that a two-impulse optimal solution occurs, we must impose constraints on impulse instants and the magnitudes of velocity impulses. Numerical solutions confirm this conjecture. Therefore, Problem 3 has been proposed. Then the static and dynamic slackness variable methods have been introduced to solve Problem 3 using MATLAB boundary value problem solvers. Numerical results showed that our method makes senses for two-impulse ballistic missile space interception problems with multiple constraints.

From the perspective of optimal control theory, numerical methods have been categorized into two approaches to solving optimization problems, i.e., indirect and direct methods. In an indirect method, an optimal solution can be obtained by satisfying a set of necessary conditions. Conversely, a direct method uses only its cost to obtain an optimal solution. Here the indirect method has been used, the advantage of which is its high solution accuracy. The shortage is also obvious; that is, almost all examples were solved by trial and error as other methods, and the initial guess of extra costate variables must be provided. We also solved a few numerical examples by direct methods (provided by the MATLAB software GPOPS version 5.0), and the same conclusions have been drawn. In addition, Conjecture 1 about the equivalence of Problem 1 and the one-impulse case remains open, which is, however, confirmed if the constraints of velocity impulses are imposed. Since the calculus of variations provides only local optimal solutions, a future research would be to investigate global optimal solutions.

Acknowledgements

We appreciate Prof. PRUSSING and Dr. SANDRIK for sharing their MATLAB scripts in Sandrik (2006). Also, thank Dr. KIERZENKA, one of the authors of these MATLAB boundary value problem solvers, for sending us his PhD dissertation (Kierzenka, 1998). We appreciate the MATLAB solvers, and without them we do not have this work.

Compliance with ethics guidelines

Li XIE, Yi-qun ZHANG, and Jun-yan XU declare that they have no conflict of interest.

References

Ben-Asher JZ, 2010. Optimal Control Theory with Aerospace Applications. American Institute of Aeronautics and Astronautics, Inc., Reston, Virginia, USA. https://doi.org/10.2514/4.867347

Bryson AE, 1980. This Week's Citation Classic. http://garfield.library.upenn.edu/classics1980/A1980JE96000001.pdf

Bryson AE, 1996. Optimal control—1950 to 1985. *IEEE Contr Syst Mag*, 16(3):26-33. https://doi.org/10.1109/37.506395

Bryson AE, Ho YC, 1975. Applied Optimal Control: Optimization, Estimation and Control. Halsted Press, New York, USA. https://doi.org/10.1201/9781315137667

Cheng GC, 1987. Guidance and Optimal Control of Ballistic Missiles. National University of Defense Technology Press, Changsha, China (in Chinese).

Colasurdo G, Pastrone D, 1994. Indirect optimization method for impulsive transfers. Proc Astrodynamics Conf on Guidance, Navigation, and Control, p.441-448. https://doi.org/10.2514/6.1994-3762

Curtis HD, 2014. Orbital Mechanics for Engineering Students (3rd Ed.). Elsevier, Oxford, UK. https://doi.org/10.1016/C2011-0-69685-1

Gobetz FW, Doll JR, 1969. A survey of impulsive trajectories. *AIAA J*, 7(5):801-834. https://doi.org/10.2514/3.5231

Han JQ, 1977. Guidance Law of Interception Problems. National Defense Industry Press, Beijing, China (in Chinese).

Hull DG, 2003. Optimal Control Theory for Applications. Springer, New York, USA. https://doi.org/10.1007/978-1-4757-4180-3

Jezewski DJ, 1975. Primer Vector Theory and Applications. NASA-TR-R-454, NASA, Washington, USA.

Kierzenka J, 1998. Studies in the Numerical Solution of Ordinary Differential Equations. PhD Thesis, Department of Mathematics, Southern Methodist University, Dallas, USA.

Kierzenka J, Shampine LF, 2001. A BVP solver based on residual control and the Matlab PSE. *ACM Trans Math Softw*, 27(3):299-316. https://doi.org/10.1145/502800.502801

Kierzenka J, Shampine LF, 2008. A BVP solver that controls residual and error. *J Numer Anal Ind Appl Math*, 3:27-41.

Lawden DF, 1964. Optimal trajectories for space navigation. *Math Gaz*, 48(36):478-479. https://doi.org/10.2307/3611765

Longuski JM, Guzmán JJ, Prussing JE, 2014. Optimal Control with Aerospace Applications. Springer, New York, USA. https://doi.org/10.1007/978-1-4614-8945-0

Luo YZ, Tang GJ, Lei YJ, et al., 2007. Optimization of multiple-impulse, multiple-revolution, rendezvous-phasing maneuvers. *J Guid Contr Dynam*, 30(4):946-952. https://doi.org/10.2514/1.25620

Luo YZ, Zhang J, Li HY, et al., 2010. Interactive optimization approach for optimal impulsive rendezvous using primer vector and evolutionary algorithms. *Acta Astronaut*, 67(3-4):396-405. https://doi.org/10.1016/j.actaastro.2010.02.014

Prussing JE, 1995. Optimal impulsive linear systems: sufficient conditions and maximum number of impulses. *J Astronaut Sci*, 43(2):195-206.

Prussing JE, 2010. Primer vector theory and applications. In: Conway BA (Ed.), Spacecraft Trajectory Optimization. Cambridge University Press, Cambridge, UK, p.16-36. https://doi.org/10.1017/CBO9780511778025

Prussing JE, Chiu JH, 1986. Optimal multiple-impulse time-fixed rendezvous between circular orbits. *J Guid Contr Dynam*, 9(1):17-22. https://doi.org/10.2514/3.20060

Qin HS, Wang CZ, 1977. Guidance Problems of Exoatmospheric Interception and Rendezvous (Collected Papers). National Defense Industry Press, Beijing, China (in Chinese).

Robinson AC, 1967. Comparison of Fuel-Optimal Maneuvers Using a Minimum Number of Impulses with Those Using the Optimal Number of Impulses: a Survey. NASA Contractor Report NASw-1146, Columbus Laboratories, Columbus, USA.

Sandrik SL, 2006. Primer-Optimized Results and Trends for Circular Phasing and Other Circle-to-Circle Impulsive Coplanar Rendezvous. PhD Thesis, University of Illinois at Urbana-Champaign, Urbana-Champaign Urbana, IL, USA.

Shampine LF, Gladwell I, Thompson S, 2003. Solving ODEs with Matlab. Cambridge University Press, Cambridge, UK. https://doi.org/10.1017/CBO9780511615542

Sigal E, Ben-Asher JZ, 2014. Optimal control for switched systems with pre-defined order and switch-dependent dynamics. *J Optim Theory Appl*, 161(2):582-591. https://doi.org/10.1007/s10957-013-0411-8

Subchan S, Żbikowski R, 2009. Computational Optimal Control: Tools and Practice. Wiley, Chichester, UK. https://doi.org/10.1002/9780470747674

Taur DR, Coverstone-Carroll V, Prussing JE, 1995. Optimal impulsive time-fixed orbital rendezvous and interception with path constraints. *J Guid Contr Dynam*, 18(1):54-60. https://doi.org/10.2514/3.56656

Tsien HS, Evans RC, 1951. Optimum thrust programming for a sounding rocket. *J Am Rocket Soc*, 21(5):99-107. https://doi.org/10.2514/8.4372

Vinh NX, Lu P, Howe RM, et al., 1990. Optimal interception with time constraint. *J Optim Theory Appl*, 66(3):361-390. https://doi.org/10.1007/BF00940927

Wang XH, Huang Y, Wang H, et al., 2014. Variable time impulse system optimization with continuous control and impulse control. *Asian J Contr*, 16(1):107-116. https://doi.org/10.1002/asjc.769

Xie L, Zhang YQ, Xu JY, 2018. Hohmann transfer via constrained optimization. *Front Inform Technol Electron Eng*, 19(11):1444-1458. https://doi.org/10.1631/FITEE.1800295

Žefran M, Desai JP, Kumar V, 1996. Continuous motion plans for robotic systems with changing dynamic behavior. Proc 2nd Int Workshop on Algorithmic Foundations of Robotics.

Appendix A: Derivation of the BCs for Problem 1

Let the symbol "$*$" as a superscript or subscript denote an optimal value. The first variation of the augmented cost functional $\delta\tilde{J}$ can be obtained as Eq. (A1) (see the next page), where we use $\mathrm{d}(\cdot)$ to denote the difference between the varied path and the optimal path taking into account the differential change in a time instant, e.g.,

$$\mathrm{d}\boldsymbol{v}(t_1^+)=\boldsymbol{v}(t_1^+)-\boldsymbol{v}^*(t_1^{+*}),$$

and $\delta(\cdot)$ is the variation; for example, $\delta\boldsymbol{v}_{\mathrm{M}}(t_1^*)$ is the variation of $\boldsymbol{v}_{\mathrm{M}}$ as an independent variable at t_1^*. The parts of $\delta\tilde{J}$ marked with "$*$" are due to the linear parts of the related integrals, and the parts of $\delta\tilde{J}$ marked with "$\dagger$" are obtained using the integration by parts.

Note that by $\delta\tilde{J}=0$ and the fundamental lemma, it follows from the related integral terms in Eq. (A1) (see the next page) that we first have the costate equation of the interceptor

$$\begin{cases}\dot{\boldsymbol{p}}_{\mathrm{M}ri}(t)=-\dfrac{\partial H_{\mathrm{M}i}(\boldsymbol{r}_{\mathrm{M}},\boldsymbol{v}_{\mathrm{M}},\boldsymbol{p}_{\mathrm{M}i})}{\partial\boldsymbol{r}_{\mathrm{M}}},\\ \dot{\boldsymbol{p}}_{\mathrm{M}vi}(t)=-\dfrac{\partial H_{\mathrm{M}i}(\boldsymbol{r}_{\mathrm{M}},\boldsymbol{v}_{\mathrm{M}},\boldsymbol{p}_{\mathrm{M}i})}{\partial\boldsymbol{v}_{\mathrm{M}}},\end{cases}$$

in the sense of optimality. In view of the definition of Hamiltonian function (11), we have

$$\begin{cases}\dot{\boldsymbol{p}}_{\mathrm{M}ri}=-\dfrac{\mu}{r_{\mathrm{M}}^3}\left(\dfrac{3}{r_{\mathrm{M}}^2}\boldsymbol{r}_{\mathrm{M}}\boldsymbol{r}_{\mathrm{M}}^{\mathrm{T}}-\boldsymbol{I}_{3\times3}\right)\boldsymbol{p}_{\mathrm{M}vi},\\ \dot{\boldsymbol{p}}_{\mathrm{M}vi}=-\boldsymbol{p}_{\mathrm{M}ri}.\end{cases}$$

For the target, there are similar costate equations. We next derive all BCs related to costates. By regrouping terms with respect to $\delta\boldsymbol{v}_0$ and $\delta\boldsymbol{v}_1$ in

$$
\begin{aligned}
\delta\tilde{J}=&\frac{\Delta\boldsymbol{v}_0^{\mathrm{T}}}{|\Delta\boldsymbol{v}_0|}\delta\boldsymbol{v}_0+\frac{\Delta\boldsymbol{v}_1^{\mathrm{T}}}{|\Delta\boldsymbol{v}_1|}\delta\boldsymbol{v}_1+\mathrm{d}\boldsymbol{r}_{\mathrm{T}}^{\mathrm{T}}(t_h)\frac{\partial\boldsymbol{g}_h(\boldsymbol{r}_{\mathrm{T}}(t_h))}{\partial\boldsymbol{r}_{\mathrm{T}}(t_h)}\Big|_*\boldsymbol{\gamma}_h+\mathrm{d}\boldsymbol{r}_{\mathrm{M}}^{\mathrm{T}}(t_h)\frac{\partial\boldsymbol{g}_h(\boldsymbol{r}_{\mathrm{M}}(t_h),\boldsymbol{r}_{\mathrm{T}}(t_h))}{\partial\boldsymbol{r}_{\mathrm{M}}(t_h)}\Big|_*\boldsymbol{\gamma}_h\\
&+\boldsymbol{q}_{v1}^{\mathrm{T}}\left[\mathrm{d}\boldsymbol{v}(t_0^+)-\mathrm{d}\boldsymbol{v}(t_0^-)-\delta\boldsymbol{v}_0\right]+\boldsymbol{q}_{v2}^{\mathrm{T}}\left[\mathrm{d}\boldsymbol{v}(t_1^+)-\mathrm{d}\boldsymbol{v}(t_1^-)-\delta\boldsymbol{v}_1\right]\\
(*)&\begin{cases}+\left(H_{\mathrm{M}1*}-\boldsymbol{p}_{\mathrm{M}r1}^{\mathrm{T}}\dot{\boldsymbol{r}}_{\mathrm{M}}-\boldsymbol{p}_{\mathrm{M}v1}^{\mathrm{T}}\dot{\boldsymbol{v}}_{\mathrm{M}}\right)\Big|_{t_1^{-*}}\delta t_1-\left(H_{\mathrm{M}2*}-\boldsymbol{p}_{\mathrm{M}r2}^{\mathrm{T}}\dot{\boldsymbol{r}}_{\mathrm{M}}-\boldsymbol{p}_{\mathrm{M}v2}^{\mathrm{T}}\dot{\boldsymbol{v}}_{\mathrm{M}}\right)\Big|_{t_1^{+*}}\delta t_1\\+\left(H_{\mathrm{M}2*}-\boldsymbol{p}_{\mathrm{M}r2}^{\mathrm{T}}\dot{\boldsymbol{r}}_{\mathrm{M}}-\boldsymbol{p}_{\mathrm{M}v2}^{\mathrm{T}}\dot{\boldsymbol{v}}_{\mathrm{M}}\right)\Big|_{t_h^{-*}}\delta t_h\end{cases}\\
(\dagger)&\begin{cases}-\boldsymbol{p}_{\mathrm{M}r1}^{\mathrm{T}}(t_1^{-*})\delta\boldsymbol{r}_{\mathrm{M}}(t_1^{-*})+\boldsymbol{p}_{\mathrm{M}r2}^{\mathrm{T}}(t_1^{+})\delta\boldsymbol{r}_{\mathrm{M}}(t_1^{+*})-\boldsymbol{p}_{\mathrm{M}r2}^{\mathrm{T}}(t_h^{-*})\delta\boldsymbol{r}_{\mathrm{M}}(t_h^{-*})\\+\boldsymbol{p}_{\mathrm{M}v1}^{\mathrm{T}}(t_0^{+})\delta\boldsymbol{v}_{\mathrm{M}}(t_0^{+})-\boldsymbol{p}_{\mathrm{M}v1}^{\mathrm{T}}(t_1^{-*})\delta\boldsymbol{v}_{\mathrm{M}}(t_1^{-*})+\boldsymbol{p}_{\mathrm{M}v2}^{\mathrm{T}}(t_1^{+*})\delta\boldsymbol{v}_{\mathrm{M}}(t_1^{+*})-\boldsymbol{p}_{\mathrm{M}v2}^{\mathrm{T}}(t_h^{-*})\delta\boldsymbol{v}_{\mathrm{M}}(t_h^{-*})\end{cases}\\
(**)&\begin{cases}+\left(H_{\mathrm{T}1*}-\boldsymbol{p}_{\mathrm{T}r1}^{\mathrm{T}}\dot{\boldsymbol{r}}_{\mathrm{T}}-\boldsymbol{p}_{\mathrm{T}v1}^{\mathrm{T}}\dot{\boldsymbol{v}}_{\mathrm{T}}\right)\Big|_{t_1^{-*}}\delta t_1\\-\left(H_{\mathrm{T}2*}-\boldsymbol{p}_{\mathrm{T}r2}^{\mathrm{T}}\dot{\boldsymbol{r}}_{\mathrm{T}}-\boldsymbol{p}_{\mathrm{T}v2}^{\mathrm{T}}\dot{\boldsymbol{v}}_{\mathrm{T}}\right)\Big|_{t_1^{+*}}\delta t_1+\left(H_{\mathrm{T}2*}-\boldsymbol{p}_{\mathrm{T}r2}^{\mathrm{T}}\dot{\boldsymbol{r}}_{\mathrm{T}}-\boldsymbol{p}_{\mathrm{T}v2}^{\mathrm{T}}\dot{\boldsymbol{v}}_{\mathrm{T}}\right)\Big|_{t_h^{-*}}\delta t_h\end{cases}\\
(\dagger\dagger)&\begin{cases}-\boldsymbol{p}_{\mathrm{T}r1}^{\mathrm{T}}(t_1^{-*})\delta\boldsymbol{r}_{\mathrm{T}}(t_1^{-*})+\boldsymbol{p}_{\mathrm{T}r2}^{\mathrm{T}}(t_1^{+})\delta\boldsymbol{r}_{\mathrm{T}}(t_1^{+*})-\boldsymbol{p}_{\mathrm{T}r2}^{\mathrm{T}}(t_h^{-*})\delta\boldsymbol{r}_{\mathrm{T}}(t_h^{-*})\\-\boldsymbol{p}_{\mathrm{T}v1}^{\mathrm{T}}(t_1^{-*})\delta\boldsymbol{v}_{\mathrm{T}}(t_1^{-*})+\boldsymbol{p}_{\mathrm{T}v2}^{\mathrm{T}}(t_1^{+*})\delta\boldsymbol{v}_{\mathrm{T}}(t_1^{+*})-\boldsymbol{p}_{\mathrm{T}v2}^{\mathrm{T}}(t_h^{-*})\delta\boldsymbol{v}_{\mathrm{T}}(t_h^{-*})\end{cases}\\
&+\int_{t_0^+}^{t_1^{-*}}\left[\left(\frac{\partial H_{\mathrm{M}1}(\boldsymbol{r}_{\mathrm{M}},\boldsymbol{v}_{\mathrm{M}},\boldsymbol{p}_{\mathrm{M}1})}{\partial\boldsymbol{r}_{\mathrm{M}}}+\dot{\boldsymbol{p}}_{\mathrm{M}r1}(t)\right)_*^{\mathrm{T}}\delta\boldsymbol{r}_{\mathrm{M}}+\left(\frac{\partial H_{\mathrm{M}1}(\boldsymbol{r}_{\mathrm{M}},\boldsymbol{v}_{\mathrm{M}},\boldsymbol{p}_{\mathrm{M}1})}{\partial\boldsymbol{v}_{\mathrm{M}}}+\dot{\boldsymbol{p}}_{\mathrm{M}v1}(t)\right)_*^{\mathrm{T}}\delta\boldsymbol{v}_{\mathrm{M}}\right]\mathrm{d}t\\
&+\int_{t_1^+}^{t_h^{-*}}\left[\left(\frac{\partial H_{\mathrm{M}2}(\boldsymbol{r}_{\mathrm{M}},\boldsymbol{v}_{\mathrm{M}},\boldsymbol{p}_{\mathrm{M}2})}{\partial\boldsymbol{r}_{\mathrm{M}}}+\dot{\boldsymbol{p}}_{\mathrm{M}r2}(t)\right)_*^{\mathrm{T}}\delta\boldsymbol{r}_{\mathrm{M}}+\left(\frac{\partial H_{\mathrm{M}2}(\boldsymbol{r}_{\mathrm{M}},\boldsymbol{v}_{\mathrm{M}},\boldsymbol{p}_{\mathrm{M}2})}{\partial\boldsymbol{v}_{\mathrm{M}}}+\dot{\boldsymbol{p}}_{\mathrm{M}v2}(t)\right)_*^{\mathrm{T}}\delta\boldsymbol{v}_{\mathrm{M}}\right]\mathrm{d}t\\
&+\int_{t_0^+}^{t_1^{-*}}\left[\left(\frac{\partial H_{\mathrm{T}1}(\boldsymbol{r}_{\mathrm{T}},\boldsymbol{v}_{\mathrm{T}},\boldsymbol{p}_{\mathrm{T}1})}{\partial\boldsymbol{r}_{\mathrm{T}}}+\dot{\boldsymbol{p}}_{\mathrm{T}r1}(t)\right)_*^{\mathrm{T}}\delta\boldsymbol{r}_{\mathrm{T}}+\left(\frac{\partial H_{\mathrm{T}1}(\boldsymbol{r}_{\mathrm{T}},\boldsymbol{v}_{\mathrm{T}},\boldsymbol{p}_{\mathrm{T}1})}{\partial\boldsymbol{v}_{\mathrm{T}}}+\dot{\boldsymbol{p}}_{\mathrm{T}v1}(t)\right)_*^{\mathrm{T}}\delta\boldsymbol{v}_{\mathrm{T}}\right]\mathrm{d}t\\
&+\int_{t_1^+}^{t_h^{-*}}\left[\left(\frac{\partial H_{\mathrm{T}2}(\boldsymbol{r}_{\mathrm{T}},\boldsymbol{v}_{\mathrm{T}},\boldsymbol{p}_{\mathrm{T}2})}{\partial\boldsymbol{r}_{\mathrm{T}}}+\dot{\boldsymbol{p}}_{\mathrm{T}r2}(t)\right)_*^{\mathrm{T}}\delta\boldsymbol{r}_{\mathrm{T}}+\left(\frac{\partial H_{\mathrm{T}2}(\boldsymbol{r}_{\mathrm{T}},\boldsymbol{v}_{\mathrm{T}},\boldsymbol{p}_{\mathrm{T}2})}{\partial\boldsymbol{v}_{\mathrm{T}}}+\dot{\boldsymbol{p}}_{\mathrm{T}v2}(t)\right)_*^{\mathrm{T}}\delta\boldsymbol{v}_{\mathrm{T}}\right]\mathrm{d}t.\quad(\mathrm{A1})
\end{aligned}
$$

Eq. (A1), we have

$$
\begin{cases}\left(\dfrac{\Delta\boldsymbol{v}_0}{|\Delta\boldsymbol{v}_0|}-\boldsymbol{q}_{v1}\right)^{\mathrm{T}}\delta\boldsymbol{v}_0,\\ \left(\dfrac{\Delta\boldsymbol{v}_1}{|\Delta\boldsymbol{v}_1|}-\boldsymbol{q}_{v2}\right)^{\mathrm{T}}\delta\boldsymbol{v}_1.\end{cases}
$$

Because $\delta\boldsymbol{v}_0$ and $\delta\boldsymbol{v}_1$ are arbitrary, their coefficients are zero. Hence, we have BCs

$$
\begin{cases}\boldsymbol{q}_{v1}-\dfrac{\Delta\boldsymbol{v}_0}{|\Delta\boldsymbol{v}_0|}=\boldsymbol{0},\\ \boldsymbol{q}_{v2}-\dfrac{\Delta\boldsymbol{v}_1}{|\Delta\boldsymbol{v}_1|}=\boldsymbol{0}.\end{cases}
$$

We use the relation between the difference $\mathrm{d}(\cdot)$ and the variation $\delta(\cdot)$, for example,

$$
\mathrm{d}\boldsymbol{v}(t_1^-)=\delta\boldsymbol{v}(t_1^{-*})+\dot{\boldsymbol{v}}(t_1^{-*})\delta t_1.\qquad(\mathrm{A2})
$$

After a careful derivation, by making the remaining coefficients of the variations of all independent variables vanish in Eq. (A1) such that $\delta\tilde{J}=0$, e.g., $(\boldsymbol{q}_{v1}+\boldsymbol{p}_{v1}(t_0^+))\mathrm{d}\boldsymbol{v}_0$, where $\mathrm{d}\boldsymbol{v}_0$ and $\mathrm{d}\boldsymbol{v}_{\mathrm{M}}(t_0^+)$ have the same meaning, we obtain the following BCs related to the costates:

$$
\begin{cases}H_{\mathrm{M}1*}(t_1^{-*})-H_{\mathrm{M}2*}(t_1^{+*})\\\quad+H_{\mathrm{T}1*}(t_1^{-*})-H_{\mathrm{T}2*}(t_1^{+*})=0,\\ H_{\mathrm{M}2*}(t_h^{-*})+H_{\mathrm{T}2*}(t_h^{-*})=0,\\ \boldsymbol{q}_{v1}+\boldsymbol{p}_{\mathrm{M}v1}(t_0^+)=\boldsymbol{0},\ \boldsymbol{q}_{v2}+\boldsymbol{p}_{\mathrm{M}v1}(t_1^{-*})=\boldsymbol{0},\\ \boldsymbol{q}_{v2}+\boldsymbol{p}_{\mathrm{M}v2}(t_1^{+*})=\boldsymbol{0},\ \boldsymbol{p}_{\mathrm{M}v2}(t_h^{-*})=\boldsymbol{0},\\ \boldsymbol{p}_{\mathrm{M}r1}(t_1^{-*})-\boldsymbol{p}_{\mathrm{M}r2}(t_1^{+*})=\boldsymbol{0},\ \boldsymbol{p}_{\mathrm{M}r2}(t_h^{-*})-\boldsymbol{\gamma}_h=\boldsymbol{0},\\ \boldsymbol{p}_{\mathrm{T}r1}(t_1^{-*})-\boldsymbol{p}_{\mathrm{T}r2}(t_1^{+*})=\boldsymbol{0},\ \boldsymbol{p}_{\mathrm{T}r2}(t_h^{-*})+\boldsymbol{\gamma}_h=\boldsymbol{0},\\ \boldsymbol{p}_{\mathrm{T}v1}(t_1^{-*})-\boldsymbol{p}_{\mathrm{T}v2}(t_1^{+*})=\boldsymbol{0},\ \boldsymbol{p}_{\mathrm{T}v2}(t_h^{-*})=\boldsymbol{0}.\end{cases}
$$

Note that the continuity of the states at t_h

implies that $\mathrm{d}\boldsymbol{r}(t_h^-)=\mathrm{d}\boldsymbol{r}(t_h^+)=\mathrm{d}\boldsymbol{r}(t_h)$ and so on. Furthermore, eliminating the intermediate quantities, e.g., $\boldsymbol{\gamma}_h$, we obtain the following BCs:

$$\begin{cases}\boldsymbol{p}_{\mathrm{M}v1}(t_0^+)+\dfrac{\Delta\boldsymbol{v}_0}{|\Delta\boldsymbol{v}_0|}=\boldsymbol{0}, \quad \boldsymbol{p}_{\mathrm{M}v1}(t_1^{-*})+\dfrac{\Delta\boldsymbol{v}_1}{|\Delta\boldsymbol{v}_1|}=\boldsymbol{0},\\ \boldsymbol{p}_{\mathrm{M}v1}(t_1^{-*})-\boldsymbol{p}_{\mathrm{M}v2}(t_1^{+*})=\boldsymbol{0}, \quad \boldsymbol{p}_{\mathrm{M}v2}(t_h^{-*})=\boldsymbol{0};\end{cases}$$

$$\begin{cases}H_{\mathrm{M1}*}(t_1^{-*})-H_{\mathrm{M2}*}(t_1^{+*})\\ \quad +H_{\mathrm{T1}*}(t_1^{-*})-H_{\mathrm{T2}*}(t_1^{+*})=0,\\ H_{\mathrm{M2}*}(t_h^{-*})+H_{\mathrm{T2}*}(t_h^{-*})=0;\end{cases}$$

$$\begin{cases}\boldsymbol{p}_{\mathrm{M}r1}(t_1^{-*})-\boldsymbol{p}_{\mathrm{M}r2}(t_1^{+*})=\boldsymbol{0},\\ \boldsymbol{p}_{\mathrm{M}r2}(t_h^{-*})+\boldsymbol{p}_{\mathrm{T}r2}(t_h^{-*})=\boldsymbol{0},\\ \boldsymbol{p}_{\mathrm{T}r1}(t_1^{-*})-\boldsymbol{p}_{\mathrm{T}r2}(t_1^{+*})=\boldsymbol{0},\\ \boldsymbol{p}_{\mathrm{T}v1}(t_1^{-*})-\boldsymbol{p}_{\mathrm{T}v2}^{\mathrm{T}}(t_1^{+*})=\boldsymbol{0},\\ \boldsymbol{p}_{\mathrm{T}v2}(t_h^{-*})=\boldsymbol{0}.\end{cases}$$

To obtain explicit BCs, we now calculate the involved Hamiltonian functions. Because

$$\begin{cases}H_{\mathrm{T2}*}(t_h^*)=\boldsymbol{p}_{\mathrm{T}r2}^{\mathrm{T}}(t_h^*)\boldsymbol{v}_{\mathrm{T}}(t_h^*)\\ \qquad\qquad -\dfrac{\mu}{r_{\mathrm{T}}^2(t_h^*)}\boldsymbol{p}_{\mathrm{T}v2}^{\mathrm{T}}(t_h^*)\boldsymbol{r}_{\mathrm{T}}(t_h^*),\\ H_{\mathrm{M2}*}(t_h^*)=\boldsymbol{p}_{\mathrm{M}r2}^{\mathrm{T}}(t_h^*)\boldsymbol{v}_{\mathrm{M}}(t_h^*)\\ \qquad\qquad -\dfrac{\mu}{r_{\mathrm{M}}^2(t_h^*)}\boldsymbol{p}_{\mathrm{M}v2}^{\mathrm{T}}(t_h^*)\boldsymbol{r}_{\mathrm{M}}(t_h^*),\end{cases}$$

we have

$$\begin{aligned}&H_{\mathrm{M2}*}(t_h^*)+H_{\mathrm{T2}*}(t_h^*)\\ &\quad=\boldsymbol{p}_{\mathrm{T}r2}^{\mathrm{T}}(t_h^*)\boldsymbol{v}_{\mathrm{T}}(t_h^*)+\boldsymbol{p}_{\mathrm{M}r2}^{\mathrm{T}}(t_h^*)\boldsymbol{v}_{\mathrm{M}}(t_h^*)\\ &\quad=\boldsymbol{p}_{\mathrm{T}r2}^{\mathrm{T}}(t_h^*)\left(\boldsymbol{v}_{\mathrm{T}}(t_h^*)-\boldsymbol{v}_{\mathrm{M}}(t_h^*)\right)\\ &\quad=\boldsymbol{p}_{\mathrm{M}r2}^{\mathrm{T}}(t_h^*)\left(\boldsymbol{v}_{\mathrm{M}}(t_h^*)-\boldsymbol{v}_{\mathrm{T}}(t_h^*)\right)=0.\end{aligned}$$

It follows from the continuity of the target state that $H_{\mathrm{T1}*}(t_1^{-*})-H_{\mathrm{T2}*}(t_1^{+*})=0$. Hence, there is

$$\begin{aligned}&H_{\mathrm{M1}*}(t_1^{-*})-H_{\mathrm{M2}*}(t_1^{+*})+H_{\mathrm{T1}*}(t_1^{-*})-H_{\mathrm{T2}*}(t_1^{+*})\\ &\quad=H_{\mathrm{M1}*}(t_1^{-*})-H_{\mathrm{M2}*}(t_1^{+*})\\ &\quad=\boldsymbol{p}_{\mathrm{M}r1}^{\mathrm{T}}(t_1^{-*})\boldsymbol{v}_{\mathrm{M}}(t_1^{-*})-\boldsymbol{p}_{\mathrm{M}r2}^{\mathrm{T}}(t_1^{+*})\boldsymbol{v}_{\mathrm{M}}(t_1^{+*})\\ &\quad=-\boldsymbol{p}_{\mathrm{M}r1}^{\mathrm{T}}(t_1^{-*})\Delta\boldsymbol{v}(t_1)=-\boldsymbol{p}_{\mathrm{M}r1}^{\mathrm{T}}(t_1^{+*})\Delta\boldsymbol{v}(t_1)\\ &\quad=0.\end{aligned}$$

We finally obtain the BCs for Problem 1 related to the costates:

$$(1)\begin{cases}\boldsymbol{p}_{\mathrm{M}v1}(t_0^+)+\dfrac{\Delta\boldsymbol{v}_0}{|\Delta\boldsymbol{v}_0|}=\boldsymbol{0},\\ \boldsymbol{p}_{\mathrm{M}v1}(t_1^{-*})+\dfrac{\Delta\boldsymbol{v}_1}{|\Delta\boldsymbol{v}_1|}=\boldsymbol{0},\\ \boldsymbol{p}_{\mathrm{M}v1}(t_1^{-*})-\boldsymbol{p}_{\mathrm{M}v2}(t_1^{+*})=\boldsymbol{0},\ \boldsymbol{p}_{\mathrm{M}v2}(t_h^{-*})=\boldsymbol{0},\\ \boldsymbol{p}_{\mathrm{M}r1}(t_1^{-*})-\boldsymbol{p}_{\mathrm{M}r2}(t_1^{+*})=\boldsymbol{0};\end{cases}$$

$$(2)\begin{cases}-\boldsymbol{p}_{\mathrm{M}r1}^{\mathrm{T}}(t_1^{-*})\Delta\boldsymbol{v}(t_1)=0,\\ \boldsymbol{p}_{\mathrm{T}r2}^{\mathrm{T}}(t_h^*)\left(\boldsymbol{v}_{\mathrm{T}}(t_h^*)-\boldsymbol{v}_{\mathrm{M}}(t_h^*)\right)=0;\end{cases}$$

$$(3)\ \boldsymbol{p}_{\mathrm{M}r2}(t_h^{-*})+\boldsymbol{p}_{\mathrm{T}r2}(t_h^{-*})=\boldsymbol{0};$$

$$(4)\begin{cases}\boldsymbol{p}_{\mathrm{T}r1}(t_1^{-*})-\boldsymbol{p}_{\mathrm{T}r2}(t_1^{+*})=\boldsymbol{0},\\ \boldsymbol{p}_{\mathrm{T}v1}(t_1^{-*})-\boldsymbol{p}_{\mathrm{T}v2}^{\mathrm{T}}(t_1^{+*})=\boldsymbol{0},\\ \boldsymbol{p}_{\mathrm{T}v2}(t_h^{-*})=\boldsymbol{0}.\end{cases}$$

The second group is from the Hamiltonian conditions. Actually, in numerical experiments, the boundary conditions (3) and (4) related to the costates of the target may not be used if we do not consider the dynamics of the target, which are just included in the BCs to provide its position and velocity. In the following, to simplify notations, the asterisk $(*)$, which denotes an optimal value, has been removed. The BCs related to the costates of the interceptor are shown in List 1.

Appendix B: Boundary conditions, parameters, and initial values for Examples 2 and 3

List 5: BCs related to the costates and inequality constraints (see the next page).

The parameters and initial values of Examples 2 and 3 are given in Tables B1 and B2, respectively. In both examples, we provide the initial guesses for velocity impulses and costates as follows:

$$\begin{cases}\mathbf{dv10}=[-300;300;-300],\\ \mathbf{dv20}=[-100;100;-100],\\ \mathbf{pmr0}=1.0\times10^{-3}[0.5396;-0.4740;0.8451],\\ \mathbf{pmv0}=[0.4862;-0.4365;0.7570].\end{cases}$$

$$
(1)\begin{cases}
\boldsymbol{p}_{\mathrm{M}v1}(t_1^-)+\dfrac{\Delta\boldsymbol{v}_1}{|\Delta\boldsymbol{v}_1|}\\
\quad+\left[\mu_1-\mu_2,\mu_3-\mu_4,\mu_5-\mu_6\right]^{\mathrm{T}}=\boldsymbol{0},\\
\boldsymbol{p}_{\mathrm{M}v2}(t_2^-)+\dfrac{\Delta\boldsymbol{v}_2}{|\Delta\boldsymbol{v}_2|}\\
\quad+\left[\mu_7-\mu_8,\mu_9-\mu_{10},\mu_{11}-\mu_{12}\right]^{\mathrm{T}}=\boldsymbol{0},\\
\boldsymbol{p}_{\mathrm{M}v1}(t_1^-)-\boldsymbol{p}_{\mathrm{M}v2}(t_1^+)=\boldsymbol{0},\\
\boldsymbol{p}_{\mathrm{M}v2}(t_2^-)-\boldsymbol{p}_{\mathrm{M}v3}(t_2^+)=\boldsymbol{0},\\
\boldsymbol{p}_{\mathrm{M}r1}(t_1^-)-\boldsymbol{p}_{\mathrm{M}r2}(t_1^+)=\boldsymbol{0},\\
\boldsymbol{p}_{\mathrm{M}r2}^{\mathrm{T}}(t_2^-)-\boldsymbol{p}_{\mathrm{M}r3}^{\mathrm{T}}(t_2^+)=\boldsymbol{0},\\
\boldsymbol{p}_{\mathrm{M}v3}(t_h^-)-\boldsymbol{p}_{\mathrm{M}v4}(t_h^+)=\boldsymbol{0};
\end{cases}
$$

$$
(2)\begin{cases}
-\boldsymbol{p}_{\mathrm{M}r1}^{\mathrm{T}}(t_1^-)\Delta\boldsymbol{v}(t_1)-\lambda_1+\lambda_2+\lambda_3=0,\\
-\boldsymbol{p}_{\mathrm{M}r2}^{\mathrm{T}}(t_2^-)\Delta\boldsymbol{v}(t_2)-\lambda_3=0,\\
\boldsymbol{p}_{\mathrm{M}r3}^{\mathrm{T}}(t_h^-)\left(\boldsymbol{v}_{\mathrm{M}}(t_h)-\boldsymbol{v}_{\mathrm{T}}(t_h)\right)=0;
\end{cases}
$$

$$
(3)\begin{cases}
\mathrm{diag}(\mu_1,\mu_3,\mu_5)\left(\Delta\boldsymbol{v}_1-\boldsymbol{p}_{1\max}\right)=\boldsymbol{0},\\
\mathrm{diag}(\mu_2,\mu_4,\mu_6)\left(\boldsymbol{p}_{1\min}-\Delta\boldsymbol{v}_1\right)=\boldsymbol{0},\\
\mathrm{diag}(\mu_7,\mu_9,\mu_{11})\left(\Delta\boldsymbol{v}_2-\boldsymbol{p}_{2\max}\right)=\boldsymbol{0},\\
\mathrm{diag}(\mu_8,\mu_{10},\mu_{12})\left(\boldsymbol{p}_{2\min}-\Delta\boldsymbol{v}_2\right)=\boldsymbol{0}.
\end{cases}
$$

Appendix C: Initial data

The examples in this paper involve three groups of initial data of the interceptor and the target generated by ballistic missiles, which are numerically obtained by corresponding orbital elements. The orbital elements of the interceptor and the target are shown in Table C1, where the orbital elements (H, i, Ω, e, and ω) denote the altitude, inclination, right ascension of the ascending node, eccentricity, and argument of perigee, respectively.

Table B1 Parameters and initial values of Example 2

Item	Value	Item	Value
α	20	$p_{4\max}$	1300
β	40	$p_{5\min}$	-1300
γ	50	$p_{5\max}$	1300
Tolerance	1×10^{-12}	$p_{6\min}$	-1300
$p_{1\min}$	-1300	$p_{6\max}$	1300
$p_{1\max}$	1300	Scaled t_1	0.04
$p_{2\min}$	-1300	Scaled t_2	0.14
$p_{2\max}$	1300	t_h	500
$p_{3\min}$	-1300	$\lambda_1,\lambda_2,\lambda_3$	1
$p_{3\max}$	1300	$\mu_1,\mu_2,\ldots,\mu_{12}$	1
$p_{4\min}$	-1300		

Table B2 Parameters and initial values of Example 3

Item	Value	Item	Value
α	20	$p_{4\max}$	400
β	40	$p_{5\min}$	-400
γ	50	$p_{5\max}$	400
Tolerance	1×10^{-12}	$p_{6\min}$	-500
$p_{1\min}$	-400	$p_{6\max}$	400
$p_{1\max}$	400	Scaled t_1	0.03
$p_{2\min}$	-400	Scaled t_2	0.1
$p_{2\max}$	400	t_h	700
$p_{3\min}$	-500	$\lambda_1,\lambda_2,\lambda_3$	1
$p_{3\max}$	400	$\mu_1,\mu_2,\ldots,\mu_{12}$	1
$p_{4\min}$	-400		

Table C1 Orbital elements

Item	First group		Second group	
	Interceptor	Target	Interceptor	Target
H (km)	500	400	500	400
i	$2\pi/3$	$\pi/6$	$2\pi/3$	$\pi/6$
Ω	$4\pi/3$	$\pi/3$	$5\pi/4$	$\pi/3$
e	0.3	0.1	0.5	0.2
ω	π	0	π	0

For the case where the true anomaly $\theta=0$, using Algorithm 4.5 in Curtis (2014), the trajectories of the interceptor and the target are known, and we then obtain the initial positions of the interceptor and the target—corresponding to the first time at which the target and the interceptor are just above the atmosphere (approximately equal to the sum of the Earth's radius 6 378 145 m and the height of the atmosphere 120 km)—and their velocities. For the first group of orbital elements, we generate initial data sets I and II, and for the second group, we have initial data set III. A reference position vector of the interceptor is chosen just above the atmosphere for initial data sets I and II (Table C2).

Appendix D: Time change

We have transformed two-impulse space interception problems into multi-point boundary value problems using the calculus of variations. To use the MATLAB boundary value problem solvers bvp4c and bvp5c, we must introduce those instants (t_1, t_2, t_h, and t_{f}) as unknown parameters because the solvers cannot directly deal with a multi-point BC value problem with unknown time interval boundary points. The solvers require the normalization of the unknown final time and the parameterization

Table C2 Initial data sets

Initial data set	Item	Value
I	Target position (m)	$1.0\times10^6[-5.842\,891\,129\,580\,837;\ -1.241\,946\,037\,180\,446;\ 2.562\,926\,625\,347\,858]$
	Target velocity (m/s)	$1.0\times10^3[-0.065\,508\,668\,182\,581;\ -7.322\,759\,468\,283\,627;\ -2.081\,144\,241\,020\,925]$
	Interceptor position (m)	$1.0\times10^6[-1.392\,985\,266\,715\,916;\ -5.682\,521\,353\,135\,304;\ -2.831\,729\,949\,288\,823]$
	Interceptor velocity (m/s)	$1.0\times10^3[-4.511\,678\,481\,085\,538;\ -2.680\,368\,719\,222\,989;\ 4.446\,250\,319\,272\,038]$
II	Target position (m)	$1.0\times10^6[-5.842\,481\,237\,484\,495;\ -1.389\,922\,138\,771\,051;\ 2.520\,004\,658\,256\,203]$
	Target velocity (m/s)	$1.0\times10^3[0.105\,801\,179\,312\,784;\ -7.284\,177\,899\,593\,129;\ -2.155\,661\,625\,234\,000]$
	Interceptor position (m)	$1.0\times10^6[-1.422\,033\,750\,436\,706;\ -5.699\,632\,649\,250\,217;\ -2.802\,976\,040\,834\,825]$
	Interceptor velocity (m/s)	$1.0\times10^3[-4.498\,532\,928\,342\,012;\ -2.627\,216\,111\,719\,469;\ 4.472\,563\,498\,532\,185]$
III	Target position (m)	$1.0\times10^6[-5.394\,452\,557\,207\,117;\ -3.192\,217\,335\,202\,957;\ 1.775\,712\,509\,707\,950]$
	Target velocity (m/s)	$1.0\times10^3[1.767\,918\,629\,073\,472;\ -6.417\,485\,911\,429\,783;\ -2.736\,527\,923\,779\,045]$
	Interceptor position (m)	$1.0\times10^6[-3.580\,084\,601\,432\,768;\ -5.106\,010\,405\,266\,481;\ -1.868\,869\,802\,369\,432]$
	Interceptor velocity (m/s)	$1.0\times10^3[-4.211\,400\,455\,599\,469;\ -0.835\,510\,934\,866\,194;\ 4.134\,603\,376\,902\,692]$
	Reference position (m)	$1.0\times10^6[-4.4528;\ -4.4166;\ 1.7258]$

of unknown time instants. For example, considering the two-impulse space interception Problem 1, we introduce a time change

$$\tau=\frac{t-t_0}{t_h-t_0},\quad t\in[t_0,t_h]. \tag{D1}$$

Then t_1, t_2, and t_h are transformed into

$$\tau_1=\frac{t_1-t_0}{t_h-t_0},\quad \tau_2=\frac{t_2-t_0}{t_h-t_0},\quad \tau_h=1. \tag{D2}$$

Then the time change (D1) transforms $[0,t_1]$ into $[0,\tau_1]$ and so on. The non-dimensional factors τ_i are called scaled time instants, which are also called scaled t_i. We now introduce the time changes for each sub-interval:

$$s=\begin{cases}\dfrac{\tau}{3\tau_1}, & \tau\in[0,\tau_1],\\ \dfrac{\tau-2\tau_1+\tau_2}{3(\tau_2-\tau_1)}, & \tau\in[\tau_1,\tau_2],\\ \dfrac{\tau-3\tau_2+2}{3(1-\tau_2)}, & \tau\in[\tau_2,1].\end{cases} \tag{D3}$$

At time t, denoting $\boldsymbol{x}=[\boldsymbol{r},\boldsymbol{v}]^{\mathrm{T}}$, $f(\boldsymbol{x})=\left[\boldsymbol{v},-\dfrac{\mu}{r^3}\boldsymbol{r}\right]^{\mathrm{T}}$, we have

$$\frac{\mathrm{d}\boldsymbol{x}}{\mathrm{d}t}=\begin{cases}f(\boldsymbol{x}), & t\in[t_0,t_1),\\ f(\boldsymbol{x}), & t\in[t_1,t_2),\\ f(\boldsymbol{x}), & t\in[t_2,t_h].\end{cases} \tag{D4}$$

With the time changes (D1)–(D3), we have

$$\frac{\mathrm{d}\boldsymbol{x}}{\mathrm{d}t}=\begin{cases}f(\boldsymbol{x}), & t\in[t_0,t_1),\\ f(\boldsymbol{x}), & t\in[t_1,t_2),\\ f(\boldsymbol{x}), & t\in[t_2,t_h],\end{cases}$$

$$\Longrightarrow\frac{\mathrm{d}\boldsymbol{x}}{\mathrm{d}s}=\begin{cases}3t_h\tau_1 f(\boldsymbol{x}), & s\in[0,1/3),\\ 3t_h(\tau_2-\tau_1)f(\boldsymbol{x}), & s\in[1/3,2/3),\\ 3t_h(1-\tau_2)f(\boldsymbol{x}), & s\in[2/3,1].\end{cases} \tag{D5}$$

After introducing the time changes, the boundary conditions at t_1 are transformed into the boundary conditions at $1/3$ and so on. Similar time changes can be applied to other problems, e.g., Problem 2, in which there are four sub-intervals. Then the solvers can be used to solve the multi-point boundary value problem of the above piecewise continuous ordinary differential equations with unknown parameters. The number of BCs is the sum of the number of sub-intervals multiplied by the number of equations and the number of unknown parameters. For time changes, we refer to, e.g., Žefran et al. (1996) and Longuski et al. (2014), for details.